Advanced Polymer Architectures with Stimuli-Responsive Properties Starting from Inimers

Katrien V. Bernaerts,[†] Charles-André Fustin,[‡] Cécile Bomal-D'Haese,[‡] Jean-François Gohy,[‡] José C. Martins,[†] and Filip E. Du Prez*,[†]

Department of Organic Chemistry, Ghent University, Krijgslaan 281 (S4-bis), 9000 Ghent, Belgium, and Unité de Chimie des Matériaux Inorganiques et Organiques (CMAT) and Research Center in Micro- and Nano-Materials and Electronic Devices (CeRMiN), Université catholique de Louvain (UCL), Place Pasteur 1, 1348 Louvain-la-Neuve, Belgium

Received November 15, 2007; Revised Manuscript Received January 20, 2008

ABSTRACT: Novel, well-defined, temperature- and/or pH-sensitive copolymer architectures were prepared by atom transfer radical (co)polymerization (ATRP) of a temperature-sensitive poly(methyl vinyl ether) (PMVE) macromonomer, obtained via living cationic polymerization of MVE initiated with inimer 3,3-diethoxypropyl acrylate. Temperature-sensitive comb architectures were obtained by ATRP homopolymerization (Me_6TREN/CuBr in toluene) of the PMVE macromonomer. ATRP copolymerization of the PMVE macromonomer with *tert*-butyl acrylate, a hydrolyzable precursor for pH-sensitive acrylic acid (AA), gives statistical graft copolymers. Palm-tree block copolymers containing a linear P*t*BA (PAA after hydrolysis) block and a branched block based on PMVE macromonomers were also prepared and fully characterized. Using turbidimetry, dynamic light scattering, FT-IR, and NMR, the temperature and/or pH responsiveness of those (co)polymer architectures are compared with the properties of previously synthesized linear block copolymers containing PMVE and P*t*BA or PAA.

Introduction

Recently, much attention has been paid to stimuli-responsive polymers that can respond reversibly to small changes in the environment (temperature, pH, ionic strength, light, electric or magnetic field, etc.), thereby resulting in a large change of a physical property (volume, structure, elasticity, etc.).[1] Those stimuli-responsive systems are of interest for various potential applications:[2] in biomedical and pharmaceutical industry (drug delivery), (bio)separations, intelligent switches and valves, sensors and actuators, etc.

In the literature, many references describe polymers sensitive to only one stimulus.[3,4] Here, we will focus on water-soluble polymers sensitive to temperature or a combination of temperature and pH. Most studies concerning pH- and temperature-sensitive multicomponent materials are concentrated on block, graft, and statistical copolymers, blends, or hydrogels of poly(meth)acrylic acid as pH-sensitive component and poly(*N*-isopropylacrylamide) or N-substituted poly(acrylamides) as temperature-sensitive segment.[5–8]

In our work, poly(acrylic acid) (PAA) was chosen as the pH-sensitive fragment and poly(methyl vinyl ether) (PMVE) as the temperature-sensitive polymer segment. PAA is a weak acidic polymer with ionizable groups ($pK_{a,apparent} = 4.75$[9]), which responds to changes in pH and ionic strength by changing coil dimensions and solubility. The electrostatic repulsion between the negatively charged carboxylic acid groups results in an increase of the hydrodynamic volume of the polymer compared to the uncharged chains at low pH. PMVE is a temperature-sensitive polymer showing reversible phase separation (lower critical solution temperature behavior, LCST) in water around body temperature (37 °C). At low temperatures, the polymer is hydrophilic and the chains extended into the aqueous solution (water-soluble). Above the cloud point temperature (T_{cp}), the polymer becomes hydrophobic, with the chains forming a compact coil and being insoluble in water.

By combining PAA and PMVE into different architectures, it is possible to vary the LCST of PMVE in a controlled manner as a function of the pH, the composition of the copolymer, and the polymer architecture. This allows to adjust the T_{cp} of the material for specific applications. However, this combination is not straightforward from a synthetic point of view because each monomer can only be polymerized via its specific mechanism.

For the polymerization of *tert*-butyl acrylate (*t*BA) (precursor for pH-sensitive acrylic acid) atom transfer radical polymerization (ATRP) was applied.[10,11] The polymerization of MVE[12] typically occurs via a living cationic mechanism starting from an acetal functionalized initiator.[13,14] Controlled polymerization techniques were selected in order to gain control over the composition, molecular weights, polydispersities, end functionalities, and thus the polymer properties.

In order to combine both living radical and living cationic polymerization, two types of heterofunctional initiators, respectively dual initiators and inimers, were used, with each type giving rise to different polymer architectures. As highlighted in a recent review,[15] a dual initiator[3,14–17] contains two initiation functions that can initiate different polymerization mechanisms selectively and independently, in such a way that the dual initiator stays attached to the growing chain. Linear block copolymers are obtained with this strategy. An inimer is characterized by the presence of an initiation function and a polymerizable group. In this paper, the synthesis and use of inimer 3,3-diethoxypropyl acrylate for the combination of ATRP and living cationic polymerization of MVE are described. First of all, the acetal initiation function will initiate living cationic polymerization of MVE in order to prepare a well-defined PMVE macromonomer, functionalized with an acrylate polymerizable group. These PMVE macromonomers will subsequently be (co)polymerized by ATRP, resulting in branched polymer architectures like comb-shaped polymers, palm-tree[18]/tadpole-shaped[19] block copolymers, and statistical graft copolymers.

In the literature, many publications about ATRP of macromonomers expressing a wide range in chemical properties[19–29]

* Corresponding author. E-mail: filip.duprez@UGent.be.
[†] Ghent University.
[‡] Université catholique de Louvain.

10.1021/ma702547g CCC: $40.75
Published on Web 03/13/2008

are available, but in many other cases it concerns copolymerizations between a normal monomer and poly(ethylene oxide) macromonomers.[30–34] In this work ATRP of PMVE macromonomers is considered, which should result in a temperature-responsive copolymer in combination with P*t*BA and a biresponsive polymer (pH and temperature) in combination with the hydrolyzed form of P*t*BA (PAA). The temperature- and/or pH-sensitive behavior of different polymer architectures with similar composition will be compared in this study using techniques such as turbidimetry, dynamic light scattering, nuclear magnetic resonance spectroscopy (NMR), and Fourier-transform infrared spectroscopy (FT-IR). Literature reports on such dual responsive behavior of PMVE and PAA have been scarce (only for blends[35–37] and hydrogels[6]) which motivates the present study.

Experimental Part

Materials and Methods. *Synthesis of Inimer 3,3-Diethoxypropyl Acrylate.* To a well-stirred solution of 3,3-diethoxy-1-propanol (10.86 mL, 69.0 mmol), 4-(dimethylamino)pyridine (0.0421 g, 0.34 mmol), and Et_3N (14.4 mL, 0.10 mol) in 250 mL of CH_2Cl_2, acryloyl chloride (5.88 mL, 72.4 mmol) was added dropwise at 0 °C. After 15 min, the reaction mixture was allowed to warm to room temperature and was subsequently stirred for 24 h. The precipitate obtained was filtered off, and the product was successively extracted with acidic ice–water (0.5 M HCl), $NaHCO_3$ (3×), brine (2×), and water (1×). After evaporation of the collected CH_2Cl_2 phases, the product was purified by column chromatography with 18:2 cyclohexane:ethylacetate as the eluent. This procedure yields 9.61 g of a transparent liquid (69% yield). ^{1}H NMR ($CDCl_3$, 300 MHz) δ (ppm): 1.20 (t, 6H, $(CH_3CH_2O)_2CH-$, $J = 7.16$ Hz), 1.98 (q, 2H, $-CHCH_2-$, $J = 6.41$ Hz), 3.51 and 3.66 (m, 4H, $CH(OCH_2CH_3)_2$), 4.25 (t, $-(C{=}O)OCH_2-$, $J = 6.40$ Hz), 4.64 (t, 1H, $-CH(OCH_2CH_3)_2$, $J = 5.84$ Hz), 5.84 (dd, 1H, $^3J = 10.36$ Hz and $^2J = 1.51$ Hz), 6.13 (dd, 1H, $^3J_1 = 10.55$ Hz and $^3J_2 = 17.33$ Hz) and 6.37 (dd, 1H, $^3J = 17.39$ Hz and $^2J = 1.50$ Hz). APT-NMR ($CDCl_3$, 75 MHz) δ (ppm): 15.28 (2C, $(CH_3CH_2O)_2CH-$), 33.07 (1C, $-CH_2CH-$), 61.02 (1C, $-(C{=}O)OCH_2CH_2-$), 61.46 (2C, $CH(OCH_2CH_3)_2$), 100.18 (1C, $-CH-$), 128.46 (1C, $CH_2{=}CH-$), 130.62 (1C, $CH_2{=}CH-$), 166.10 (1C, $-(C{=}O)O-$). GC-MS (*m*/*z*): 157 $[M - OCH_2CH_3]^+$; 103; 85; 57; 55; 47. Thin-layer chromatography with 18:2 cyclohexane:ethylacetate as eluent gives a ratio to front of 0.28 (developed with I_2 on silica). Anal. Calcd for $C_{10}H_{18}O_4$ (202.248 g/mol): C (59.39%) H (8.97%) O (31.64%). Found: C (59.62%) H (8.82%) Br (31.29%).

Synthesis of Acrylate-Functionalized PMVE Macromonomer (PMVE-A). A typical polymerization procedure for $[monomer]_0/[initiator]_0 = 15.3$ is given below: 5.38 mL (26.2 mmol) 3,3-diethoxypropyl acrylate and 4.48 mL (31.5 mmol) trimethylsilyl iodide (TMSI) were added to 230 mL of dry toluene under a nitrogen atmosphere at −40 °C. After 10 min, an initial amount of MVE (1.50 g, 0.025 mol) was added. The polymerization was started by the addition of activator ZnI_2 (279 mg, 0.874 mmol, dissolved in 10 mL diethyl ether). At the same moment, the addition of MVE gas was continued at a rate of 50 g/h until the desired $[monomer]_0/[initiator]_0$ ratio was achieved (total 23.3 g, 0.401 mol). After 55 min, the reaction (still at −40 °C) was terminated by the addition of $LiBH_4$ (2 M in THF) (15.7 mL, 31.5 mmol), and the excess of $LiBH_4$ was destroyed by the addition of water. The polymer solution was washed three times with 10% aqueous $Na_2S_2O_3$ and then three times with deionized water and dried over $MgSO_4$. Next, the solution is filtered and toluene was removed using a cold trap and under vacuum (oil pump). The resulting yellow viscous oil (yield: 79%) was stored in a freezer, protected from the light by aluminum foil in order to avoid autopolymerization. $M_{n,GPC}$(PMVE-A) = 1300 g/mol and $M_w/M_n = 1.12$ ($CHCl_3$ as eluent, polystyrene standards); $M_{n,NMR} = 1100$ g/mol; $M_{n,MALDI} = 1050$ g/mol. The average polymerization degree of MVE is 16, which is represented by a subscript: $PMVE_{16}$-A. ^{1}H NMR (300 MHz, $CDCl_3$) δ (ppm): 1.18 (t, 3H, $-OCH_2CH_3$), 1.34–2.04 ($2H_{polymer}$ namely CH_2 protons of PMVE and $2H_{inimer}$ $-CH_2CH_2CH-$), 3.14–3.74 (broad, $4H_{polymer}$ namely $CH-$ and CH_3 protons of PMVE and $3H_{inimer}$, namely $-CH_2CH(OCH_2CH_3)-$), 4.28 (t, 2H, $-OCH_2-$), 5.83 (dd, 1H $CH_2{=}CH-$), 6.13 (dd, 1H $CH_2{=}CH-$), 6.37 (dd, 1H $CH_2{=}CH-$). FT-IR (KBr, CH_2Cl_2) ν (cm^{-1}): 2950–2820 (s), 1726 (m) (C=O, ester of initiator), 1636 (w) (ν C=C), 1458 (w), 1378 (w), 1294 and 1272 (w), 1190, 1106, and 1078 (s) (ν_{as} C−O−C), 983 and 813 (w) (CH-bending double bond).

ATRP Homopolymerization of PMVE-A Macromonomer (Poly(PMVE$_{16}$)$_{23}$ in Table 2). 0.60 g of $PMVE_{16}$-A (0.55 mmol), 1.77 μL of ethyl-2-bromopropionate ($1.36\ 10^{-2}$ mmol), 3.49 μL of Me_6TREN (1.36×10^{-2} mmol), and 0.35 mL of toluene were mixed in a test tube using a stirring bar. The reaction mixture was degassed via three freeze–pump–thaw cycles, and 2.00 mg (1.36×10^{-2} mmol) of CuBr was added to the frozen reaction mixture under nitrogen. The tube was subsequently sealed with a septum, and all residual oxygen was removed under vacuum. The reaction mixture was allowed to thaw and put under nitrogen, and the reaction was started by immersing the tube in a preheated oil bath at 90 °C. The reaction was terminated in liquid nitrogen after 225 min (58% conversion). After dilution with THF, the catalyst was removed with Al_2O_3. In order to remove unreacted macromonomer (42%), the THF solution was dialyzed against water with a Spectra/Por 7 dialysis membrane (molecular weight cutoff of 1000 g/mol) for 10 days, with replacement of the water at regular time intervals. The final polymer (light yellow, viscous) is obtained after lyophilization of the aqueous solution present inside the dialysis membrane. GPC analysis confirms that the unreacted macromonomer has disappeared (no more low molecular weight peak). ^{1}H NMR (300 MHz, $CDCl_3$) δ (ppm): 1.16 (broad, 12H, $-C(CH_3)_2$ and $2 \times CH_3CH_2O-$), 1.40–2.10 ($4H_{polymer}$ namely CH_2 protons of PMVE and CH_2 protons of the acrylate backbone of the polymacromonomer; $2H_{inimer}$ $-CH_2CH_2CH-$), 2.23 (broad, 1H, CH protons of the acrylate backbone of the polymacromonomer), 3.14–3.73 (broad, 4H polymer namely $CH-$ and CH_3 protons of PMVE and $3H_{inimer}$, namely $-CH_2CH(OCH_2CH_3)-$), 4.12 (broad, $2H_{polymer}$ and $2H_{initiator}$, $-OCH_2-$). FT-IR (KBr, CH_2Cl_2) ν (cm^{-1}): 2950–2821 (s), 1732 (s) (C=O, ester), 1463 (m), 1455 (m), 1380 (m), 1261 (m), 1186 (m), 1103 and 1023 (s) (ν_{as} C−O−C), 867 (w), 800 (s). $M_{n,GPC} = 13\,800$ g/mol and $M_w/M_n = 1.15$ ($CHCl_3$ as solvent, polystyrene standards).

Synthesis of PtBA-Br Macroinitiators by ATRP. P*t*BA-Br macroinitiators were prepared by ATRP using methyl-2-bromopropionate/Me_6TREN/CuBr, as described by Du Prez et al.[38] (see Table 1).

Table 1. Data for Br-Terminated P*t*BA Obtained by ATRP

code[b]	$M_{n,GPC}$ (g/mol)[c]	M_w/M_n[a]	$M_{n,NMR}$ (g/mol)
$PtBA_{23}$	2850	1.10	3100
$PtBA_{51}$	6900	1.08	6700

[a] M_n = number-average molecular weight; M_w = weight-average molecular weight; M_w/M_n = polydispersity index. [b] Subscripts represent the degree of polymerization. [c] GPC with refractive index detection in $CHCl_3$, calibrated with polystyrene standards.

Statistical Graft Copolymers Poly(tBA-co-PMVE$_{16}$-A) by ATRP Copolymerization of tBA and PMVE$_{16}$-A. For poly(*t*BA-*co*-$PMVE_{16}$), **8** (see Table 3), with an initial monomer mixture of 90/10 mol % *t*BA/$PMVE_{16}$-A ($DP_{tBA} = 270$), 0.425 g (0.387 mmol) of $PMVE_{16}$-A was weighed in a test tube containing a magnetic stirring bar. 0.505 mL (3.48 mmol) of *t*BA, 1.67 μL (0.0129 mmol) of ethyl 2-bromopropionate initiator, 6.59 μL (2.58×10^{-2} mmol) of Me_6TREN ligand, and 2.47 mL of toluene were added. The reaction mixture was degassed by five freeze–pump–thaw cycles, and 3.70 mg (2.58×10^{-2} mmol) of CuBr was added under a nitrogen atmosphere to the frozen reaction mixture. Next, the tube was sealed with a septum, and residual oxygen above the frozen reaction mixture was removed by pumping. The reaction mixture was allowed to thaw and was immersed in a preheated oil bath at 90 °C. After 120 min (% conversion *t*BA = 94 and % conversion $PMVE_{16}$-A = 83), the reaction was terminated by cooling in liquid

Table 2. Results of the ATRP Homopolymerization of PMVE-A Macromonomers in Toluene, Initiated with Ethyl 2-Bromopropionate

code[a]	$PMVE_{16}$-A/ EtBrPr/CuBr/Me_6TREN	*T* (°C)	toluene (wt %)	time (min)	% conversion[b]	$M_{n,conv}$[c] (g/mol)	$M_{n,GPC}$[d] (g/mol)	M_w/M_n[d]
$poly(PMVE_{14})_{12}$	20:1:0.7:0.7	90	38	279	62	12 300	9 500	1.09
$poly(PMVE_{16})_{17}$	40:1:1:1	50	33	275	44	19 200	14 100	1.08
$poly(PMVE_{16})_{23}$	40:1:1:1	90	33	225	58	25 300	13 800	1.15

[a] Subscripts represent the degree of polymerization (DP) obtained by $DP_{PMVE\text{-}A} = DP_{theoretical} \times$ % conversion. [b] % conversion from refractive index vs retention time via GPC ($CHCl_3$, polystyrene standards) (see Supporting Information, Figure S1). [c] $M_{n,conv} = DP_{theoretical} \times M_n$(PMVE-A) × (% conversion). [d] GPC with refractive index detection in $CHCl_3$, calibrated with polystyrene standards.

Table 3. Results for the ATRP Copolymerizations of *t*BA with $PMVE_{16}$-A (MM) in Toluene at 90 °C

$poly(tBA\text{-}co\text{-}PMVE_{16})$	*t*BA/ $PMVE_{16}$-A/ EtBrPr/ CuBr/ Me_6TREN	f^a *t*BA/MM (mol %)	F^a *t*BA/MM (mol %)[b]	conc. monomer (mol/L)	wt % toluene	time (min)	% conversion *t*BA/ PMVE	$M_{n,GPC}$ (g/mol)[e]	M_w/M_n[e]
1	13/38/1/0.75/0.75	25/75	37/63	1.5	39	180	58/52[c]	12 950	1.13
2	25/25/1/0.75/0.75	50/50	56/44	1.4	47	90	75/67[c]	12 100	1.16
3	25/25/1/1/1	50/50	58/42	2.2	35	60	94/88[c]	14 500	1.21
4	38/13/1/0.75/0.75	75/25	79/21	1.3	60	165	89/80[c] 87/81[d]	9 600	1.26
5	30/270/1/2/2	10/90	18/82	1.5	36	260	78/65[c] 80/67[d]	17 300	1.21
6	30/270/1/2/2	10/90	15/85	2.6	24	74	43/32[c]	13 000	1.07
7	270/30/1/2/2	90/10	—[f]	1.4	69	169	36/28[c] 36/28[d]	19 800	1.15
8	270/30/1/2/2	90/10	92/8	5.1	20	120	94/83[c]	44 200	1.33

[a] *f* = molar fraction of comonomers in the feed; *F* = molar fractions of monomers in the copolymer. [b] From ^{1}H NMR: mol % P*t*BA = [$9H_{PtBA}$(δ = 1.4 ppm)/9]/[$4H_{PMVE}$(δ = 3.4 ppm)/($4DP_{PMVE\text{-}A}$)] × 100 and mol % PMVE = 100 − mol % P*t*BA. [c] % conversion for *t*BA from GC and % conversion for the macromonomer from GPC after correction for the contribution of P*t*BA via Gladstone−Dale. [d] % conversion from ^{1}H NMR by comparison of a monomer peak (δ = 5.79–5.86 ppm for PMVE-A and δ = 5.69–5.77 ppm for *t*BA) with toluene as an internal standard (3H at 7.12–7.22 ppm). [e] Determined via GPC ($CHCl_3$, refractive index detection, polystyrene standards). [f] Not determined.

Table 4. Results for the ATRP of $PMVE_{16}$-A Macromonomers in Toluene, Initiated with P*t*BA-Br-Macroinitiators

code[a]	$PMVE_{16}$-A/P*t*BA-Br/ Me_6TREN/ CuBr/$CuBr_2$	*T* (°C)	solvent (wt %)	time (min)	% conversion[b]	$M_{n,conv}$[c] (g/mol)	mol % P*t*BA[d]	$M_{n,GPC}$[e] (g/mol)	M_w/M_n[e]
$PtBA_{23}$-*b*-$poly(PMVE_{16})_{14}$	40/1/1/1/0	50	33% acetone	330	36	19 200	62	12 700	1.07
$PtBA_{23}$-*b*-$poly(PMVE_{16})_{18}$	40/1/1/1/0	90	33% toluene	279	46	22 900	56	13 000	1.11
$PtBA_{23}$-*b*-$poly(PMVE_{16})_{32}$	40/1/2/2/0	90	33% acetone	256	80	38 300	46	17 900	1.19
$PtBA_{23}$-*b*-$poly(PMVE_{16})_{7.5}$	10/1/2/2/0.1	90	33% toluene	38	75	11 400	76	8 600	1.19
$PtBA_{51}$-*b*-$poly(PMVE_{16})_{17}$	40/1/2/2/0	90	33% toluene	173	42	25 200	75	15 000	1.16
$PtBA_{51}$-*b*-$poly(PMVE_{16})_{26}$	30/1/3/3/0	90	33% toluene	172	65	28 000	74	15 100	1.18

[a] $DP_{PMVE\text{-}A} = DP_{theoretical} \times$ % conversion. [b] % conversion from ^{1}H NMR by comparison of a macromonomer peak (δ = 5.79–5.86 ppm) with toluene (3H at 7.12–7.22 ppm) as an internal standard. [c] $M_{n,conv} = DP_{theoretical} \times$ (% conversion) × M_n($PMVE_{16}$-A). [d] mol % P*t*BA from ^{1}H NMR. [e] Determined by GPC with $CHCl_3$ as an eluent, refractive index detection, and calibration with polystyrene standards.

nitrogen, the polymer was diluted with THF, and the catalyst was removed with neutral Al_2O_3. In order to remove unreacted (macro)-monomer (6% unreacted *t*BA, 17% unreacted $PMVE_{16}$-A), the colorless THF solution was dialyzed against water (replaced repeatedly) with a Spectra/Por 7 dialysis membrane with a molecular weight cutoff of 1000 g/mol (at room temperature for 10 days). The polymer was finally isolated as a colorless, transparent, viscous polymer by lyophilization of the aqueous solution. GPC analysis confirmed that the unreacted macromonomer was efficiently removed. ^{1}H NMR ($CDCl_3$, 300 MHz) δ (ppm): 1.16 (broad, 9H, 2 × CH_3CH_2O−, −O(C═O)CH(CH_3)−), 1.43 (s, 9H, C(CH_3)$_3$ protons of P*t*BA), 1.49–2.01 (broad, $6H_{polymer}$ namely CH_2 protons of PMVE, CH_2 protons of P*t*BA and CH_2 protons of the acrylate backbone of the polymacromonomer; $2H_{inimer}$ −CH_2CH_2CH−), 2.27 (s, $2H_{polymer}$ namely C*H* protons of P*t*BA and C*H* protons of the acrylate backbone of the polymacromonomer, $1H_{initiator}$ −O(C═O)C*H*(CH_3)−), 3.13–3.73 (broad, $4H_{polymer}$ namely C*H* and CH_3 protons of PMVE, $3H_{inimer}$ namely −CH_2CH(OCH_2CH_3)− and CH_3CH_2O−), 4.12 (s, CH_2O(C═O)− of the inimer and initiator and R_2C*H*Br). FT-IR (KBr, CH_2Cl_2) ν (cm^{-1}): 2975–2820 (m), 1729 (s) (C═O, ester), 1456 (w), 1392 and 1367 (m) (asymmetric doublet for tertiary butyl groups), 1256 (w), 1150 and 1108 (s) (ν_{as} C−O−C). $M_{n,GPC}$[poly(*t*BA-*co*-$PMVE_{16}$-A) **8**] = 44 200 g/mol and M_w/M_n = 1.33; mol % P*t*BA by ^{1}H NMR is 92%.

Synthesis of $PtBA_{51}$-b-$poly(PMVE_{16})_{17}$ via ATRP of $PMVE_{16}$-A Starting from a Br-Terminated PtBA Macroinitiator (Table 4). 0.585 g of $PMVE_{16}$-A (0.532 mmol), 1.33×10^{-2} mmol of macroinitiator (0.0891 g of $PtBA_{51}$-Br), 6.80 μL of Me_6TREN (2.66×10^{-2} mmol), and 0.37 mL of solvent (toluene) were added to a test tube with stirring bar. The reaction mixture was degassed by three freeze–pump–thaw cycles, and 2.60 mg of CuBr (2.65×10^{-2} mmol) was added to the frozen reaction mixture. The tube was subsequently sealed with a septum, and all residual oxygen was removed under vacuum. The reaction mixture was allowed to thaw and put under nitrogen, and the reaction was started by immersing the tube in a preheated oil bath at 90 °C. After the desired reaction time (173 min and 42% conversion for $PtBA_{51}$-*b*-$poly(PMVE_{16})_{17}$), the reaction mixture was terminated by cooling in liquid nitrogen and by dilution with THF. Catalyst was removed over Al_2O_3, and the THF solution was dialyzed against water with Spectra/Por 7 dialysis membranes (molecular weight cutoff of 1000 g/mol) for 10 days in order to remove unreacted macromonomer (58%). The water was replaced at regular time intervals. The final polymer (colorless, transparent, viscous) was isolated by lyophilization of the water inside the dialysis membrane. GPC analysis confirms that the unreacted macromonomer was efficiently removed. ^{1}H NMR (300 MHz, $CDCl_3$) δ (ppm): 1.16 (broad, 6H, −C(═O)CH(CH_3)− and CH_3CH_2O−), 1.44 (broad, 9H, −C(CH_3)$_3$ protons of P*t*BA), 1.48–2.02 ($6H_{polymer}$ namely CH_2 protons of PMVE, CH_2 protons of the acrylate backbone of the polymacromonomer and CH_2 protons of P*t*BA; $2H_{inimer}$ −CH_2CH_2CH−), 2.24 (broad, $2H_{polymer}$, C*H* protons of the acrylate backbone of the polymacromonomer and C*H* protons of P*t*BA), 3.12–3.63 (broad, $4H_{polymer}$ namely C*H* and CH_3 protons of PMVE and $3H_{inimer}$, namely −CH_2CH(OCH_2CH_3)−), 4.11 (broad, R_2CHBr, $2H_{polymer}$ −OCH_2− and $3H_{initiator}$ −OCH_3). FT-IR (KBr, CH_2Cl_2) ν (cm^{-1}): 2974–2820 (s), 1731 (vs) (C═O, ester), 1455 (m), 1383 and 1368 (asymmetric doublet for tertiary butyl groups), 1254 (m), 1141 (s), 1102 and 1085 (s) (ν_{as} C−O−C), 843 (w), 792 (s). $M_{n,GPC}$[$PtBA_{51}$-*b*-$poly(PMVE_{16})_{17}$] = 15 000 g/mol and M_w/M_n = 1.16 ($CHCl_3$ as

Scheme 1. Schematic Representation of the Inimer Strategy To Combine Living Cationic Polymerization and ATRP (A) Living Cationic Polymerization of MVE with Inimer 3,3-Diethoxypropyl Acrylate, (B) ATRP Homopolymerization of PMVE-A, (C) ATRP Block Copolymerization of PMVE-A Initiated with P*t*BA-Br Macroinitiator, and (D) Statistical ATRP Copolymerization of PMVE-A and *t*BA[a]

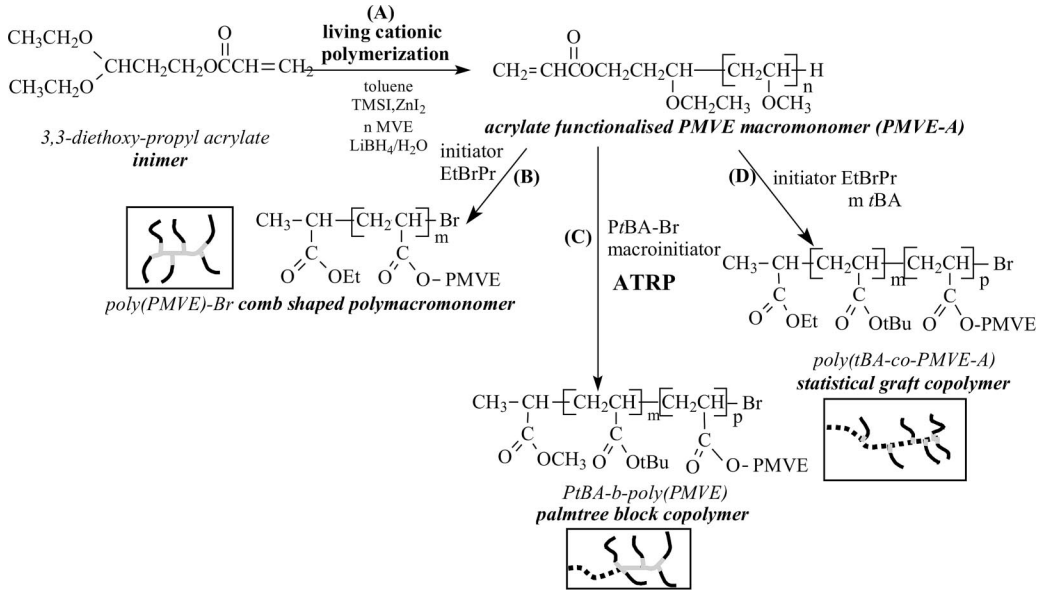

[a] Legend: gray = inimer, black = PMVE, dotted line = P*t*BA.

eluent, polystyrene standards); mol % P*t*BA by ^{1}H NMR is 75%.

Hydrolysis of PtBA in PtBA-b-polyPMVE and Poly(tBA-co-PMVE). Statistical graft copolymers (poly(*t*BA-*co*-PMVE)) and palm-tree block copolymers (P*t*BA-*b*-poly(PMVE)) were hydrolyzed with a 5-fold excess of $MeSO_3H$ relative to the *tert*-butyl ester groups for 1 h in CH_2Cl_2 (1 mL per g of copolymer). This procedure is exemplified for the hydrolysis of poly(*t*BA-*co*-$PMVE_{16}$) **8**.

0.70 g of poly(*t*BA-*co*-$PMVE_{16}$) **8** with 56 wt % P*t*BA (Table 3) was hydrolyzed in 7 mL of CH_2Cl_2 at room temperature for 1 h with a 5-fold excess of $MeSO_3H$ with respect to the *tert*-butyl ester groups (0.989 mL, 15.2 mmol). The reaction mixture was subsequently purified by dialysis in water with a Spectra/Por 7 dialysis membrane with a molecular weight cutoff of 1000 g/mol (at room temperature for 2 days). Poly(AA-*co*-$PMVE_{16}$) **8** was finally isolated as a yellow to brown polymer (0.47 g) by lyophilization of the aqueous solution. Full conversion of P*t*BA to PAA was obtained, as confirmed by ^{1}H NMR (disappearance of the typical *tert*-butyl resonance at 1.44 ppm) and FT-IR data (disappearance of the typical *tert*-butyl asymmetric doublet at 1392 and 1367 cm^{-1} (m)). ^{1}H NMR ($CDCl_3$, 300 MHz) δ (ppm): 1.17 ($3H_{inimer}$ CH_3CH_2O-, and $6H_{initiator}$ namely CH_3O- and $-O(C{=}O)CH(CH_3)-$), 1.45–2 (broad, $6H_{polymer}$ namely CH_2 protons of PAA, CH_2 protons of PMVE and CH_2 protons of the acrylate backbone of the polymacromonomer; $2H_{inimer}$ $-CH_2CH_2CH-$), 2.40 (s, $2H_{polymer}$, C*H* protons of PAA and C*H* protons of polymacromonomer backbone; $1H_{initiator}$ $-O(C{=}O)CH(CH_3)-$), 3.02–3.70 (broad, $4H_{polymer}$, C*H* and CH_3 protons of PMVE; $3H_{inimer}$, namely $-CH(OCH_2CH_3)-$), 4.14 (s, 5H, 2 × $-CH_2OC{=}O-$ and R_2CHBr). FT-IR (KBr pellets pressed) ν (cm^{-1}): 3700–2300 (broad) (complexed COOH), 1732 (vs), 1450 (m), 1365 (w), 1244–1176 (m) (ν_{as} C−O−C), 1109 (w), 1054 (m), 954, 924, and 884 (w).

Results and Discussion

The combination of living cationic polymerization of MVE and controlled radical polymerization using an inimer is based on a two-step strategy (Scheme 1). In a first step (Scheme 1A), the acetal function of the inimer 3,3-diethoxypropyl acrylate is used to initiate MVE polymerization, giving rise to PMVE with a polymerizable acrylate end group (PMVE macromonomer, PMVE-A). The macromonomer obtained is subsequently polymerized by ATRP. Comb-shaped polymers are the result of the homopolymerization of the macromonomers (Scheme 1B). Statistical copolymerization of PMVE-A with *t*BA leads to graft copolymers with an acrylate backbone and PMVE grafts (Scheme 1D). When a linear polymer such as P*t*BA-Br, obtained by ATRP, is used as a macroinitiator for the polymerization of a macromonomer, a block copolymer arises with a branched second block. These types of block copolymers are also called palm-tree block copolymers[18] or tadpole-shaped[19] block copolymers (Scheme 1C).

Synthesis of Acrylate-Functionalized Poly(methyl vinyl ether) Macromonomer (PMVE-A) by Living Cationic Polymerization of MVE. An acrylate-functionalized PMVE macromonomer (PMVE-A) was prepared by living cationic polymerization of MVE in toluene with 3,3-diethoxypropyl acrylate/trimethylsilyl iodide (TMSI) as initiating system and ZnI_2 as activator at −40 °C, which is known to produce living vinyl ether polymers[13,14] (Scheme 1A). The polymerization was deactivated by adding $LiBH_4$ in order to convert the α-iodo ether ends into nonreactive proton groups. Functional initiator 3,3-diethoxypropyl acrylate containing both an initiation function for living cationic polymerization of MVE (acetal) and a polymerizable vinyl group (acrylate monomer) (inimer) was used to introduce the polymerizable group in the macromonomer. The results for the synthesis of the PMVE-A macromonomer are given in the Experimental Part. Since the PMVE-A will be used as macromonomer, the preservation of the acrylate functionality during living cationic polymerization is essential. The end-group functionality was verified by MALDI-TOF. The molecular weight difference between two consecutive peaks in the MALDI spectrum (Figure 1a) is 58 Da, which corresponds to the mass of one MVE monomer unit. Figure 1b presents the m/z = 819–882 Da range of this spectrum in more detail. The MALDI-TOF spectrum is used for determination of chain-end structures, by comparison of experimental (top) and simulated (bottom) isotope distributions (Figure 1b). The good correspondence of the shape of both isotopical patterns and of the m/z values confirms that the desired fully acrylate-

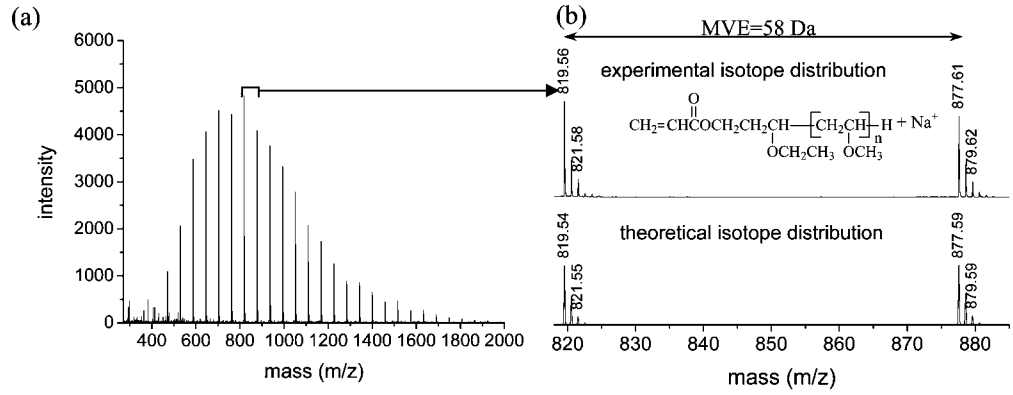

Figure 1. (a) Reflectron mode MALDI-TOF of $PMVE_{16}$-A and (b) determination of end groups for $PMVE_{16}$-A, by comparison of experimental (top) and theoretical (bottom) isotope distributions.

functionalized PMVE was synthesized, without any trace of side product.

ATRP Homopolymerization of PMVE-A Macromonomer. Before proceeding to the ATRP synthesis of (block) copolymers starting from PMVE-A macromonomer, the reaction conditions are investigated for the ATRP homopolymerization of PMVE-A initiated with ethyl 2-bromopropionate (Scheme 1B). As the PMDETA/CuBr catalyst systems did not result in any polymerization, we switched to the more active Me_6TREN/CuBr catalyst system (giving a higher equilibrium constant),[39] often used for ATRP of acrylates (Table 2). A more active catalyst system was required because the concentration of reactive sites in the solution is relatively low since the macromonomer itself is of relatively high molecular weight.

Using the reaction conditions in Table 2, it was not possible to achieve full conversion (determined by GPC, see Supporting Information, Figure S1) of the macromonomer. The highest conversion could be obtained when the lowest degree of polymerization was targeted. This since the radical concentration is the highest, the viscosity limited and the effect of steric hindrance around the growing radical are less pronounced. If a higher degree of polymerization (DP = 40) is targeted, the reaction stops at slightly lower conversions, although a higher catalyst concentration was used to increase the concentration of radicals in the solution and enhance the rate of the polymerization. The results in Table 2 and the first-order kinetic plot in Figure 2a further show that the system reactivity (and thus the conversion) could be influenced by the reaction temperature: an increase of the temperature from 50 °C ($poly(PMVE_{16})_{17}$) to 90 °C ($poly(PMVE_{16})_{23}$), corresponds to an increase of the conversion from 44% to 58%. The kinetic study further shows that the reaction is controlled up to a certain conversion, after which deviation in the first-order kinetic plot is observed (Figure 2a). Nevertheless, the polymers obtained have a narrow molecular weight distribution and M_n evolves linearly as a function of the conversion (Figure 2b). Similar deviations of the first-order kinetics were already mentioned earlier in literature for the radical polymerization of macromonomers. They were ascribed to the increasing viscosity of the reaction medium and/or to increasing steric hindrance around the propagating species, rather than to irreversible termination reactions like the recombination of growing radicals.[20]

It has been reported previously for the controlled radical polymerization of sterically hindered 4-acetoxystyrene[40] and for the controlled homopolymerization of macromonomers (poly(isobutyl vinyl ether),[20] poly(tetrahydrofuran),[21] poly(lactic acid),[22] poly(dimethylsiloxane),[24–26] etc.) that, as the polymerization proceeds and the viscosity of the medium increases, the propagation mechanism can change from a chemically controlled to a diffusion-controlled process. However, Roos et al.[41] indicated that for controlled radical (co)polymerization the diffusion phenomenon was less pronounced than for free radical polymerization because the time interval for monomer addition to a polymer chain is much larger (seconds or minutes) than for conventional radical systems (milliseconds).

However, more recently, Ohno et al.[19] ascribed the limited degree of polymerization of macromonomers to progressively increasing steric congestion for macromonomers in approaching the growing chain ends of densely grafted polymers. High segment density around the propagating chain end makes it more difficult for the active site to approach the polymerizable end group of the macromonomers. The effect of steric hindrance increases as the number of branches around the propagating active place increases.[42] As the segment density around the propagating radical increases at high conversion, bimolecular termination becomes more difficult. By consequence, initial termination reactions are more important with the polymerization of macromonomers.[43]

Statistical Graft Copolymers Based on PMVE-A Macromonomers and *t*BA: Poly(PMVE-A-co-*t*BA). ATRP copolymerization of two acrylates, namely *t*BA and PMVE-A macromonomer, was performed with EtBrPr as an initiator, in toluene as a solvent (Scheme 1C). The results of the copolymerizations are shown in Table 3.

The conversion of the PMVE-A macromonomer was determined by GPC from the peak area of the original macromonomer compared to the peak area of the copolymer (after deconvolution when appropriate). The apparent GPC peak areas were corrected for the contribution of the *t*BA conversion (measured by GC). This procedure was derived from the relationship between polymer concentrations and their relative intensities in the GPC signal. If the densities of the polymers are comparable ($\rho_{20\ °C}$(PMVE) = 1.058 g/cm^3; ρ(P*t*BA) = 1.022 g/cm^3),[44] the signal intensities of PMVE and of the PMVE/P*t*BA copolymers can be approximated in GPC, using the Gladstone−Dale equation (1),[45,46] which states the additivity of the refractive indices of the constituent components in copolymers.

$$\frac{\text{GPC area}_{PMVE_{16}\text{-A}}}{\text{GPC area}_{\text{copolymer}}} = \{[PMVE_{16}\text{-A}]_0 MW_{PMVE_{16}\text{-A}}(1 - \text{conversion}_{PMVE_{16}\text{-A}})R_1\} \Big/ \{([PMVE_{16}\text{-A}]_0 MW_{PMVE_{16}\text{-A}} \cdot \text{conversion}_{PMVE_{16}\text{-A}} \cdot R_1) + ([t\text{BA}]_0 MW_{t\text{BA}} \cdot \text{conversion}_{t\text{BA}} \cdot R_2)\} \quad (1)$$

with $R_1 = n_D$(PMVE) − n_D($CHCl_3$), $R_2 = n_D$(P*t*BA) − n_D($CHCl_3$), n_D($CHCl_3$) = 1.444, n_D(PMVE) = 1.467, and

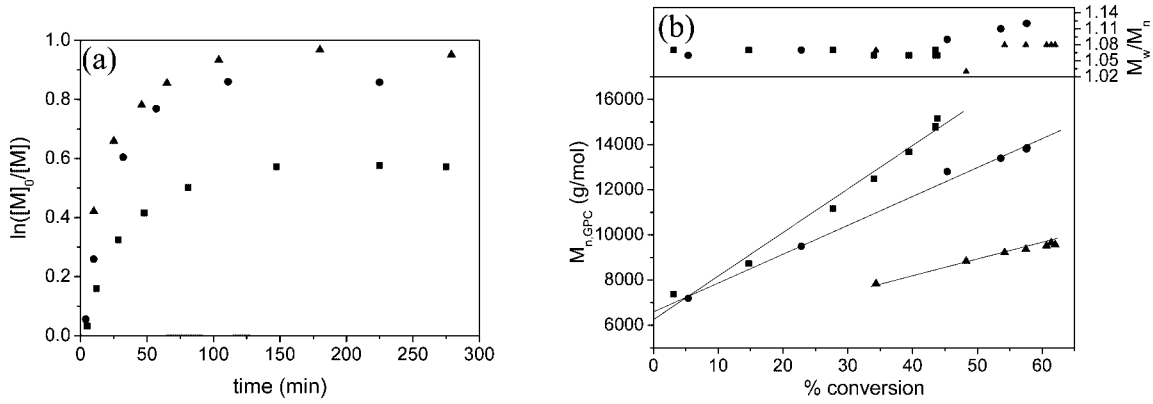

Figure 2. Kinetic curves of (a) $\ln([M]_0/[M])$ vs reaction time and (b) dependence of $M_{n,GPC}$ (bottom) and molecular weight distributions (top) of the monomer conversion for ATRP of PMVE-A: poly($PMVE_{14}$)$_{12}$ (▲), poly($PMVE_{16}$)$_{17}$ (■), and poly($PMVE_{16}$)$_{23}$ in Table 2 (●).

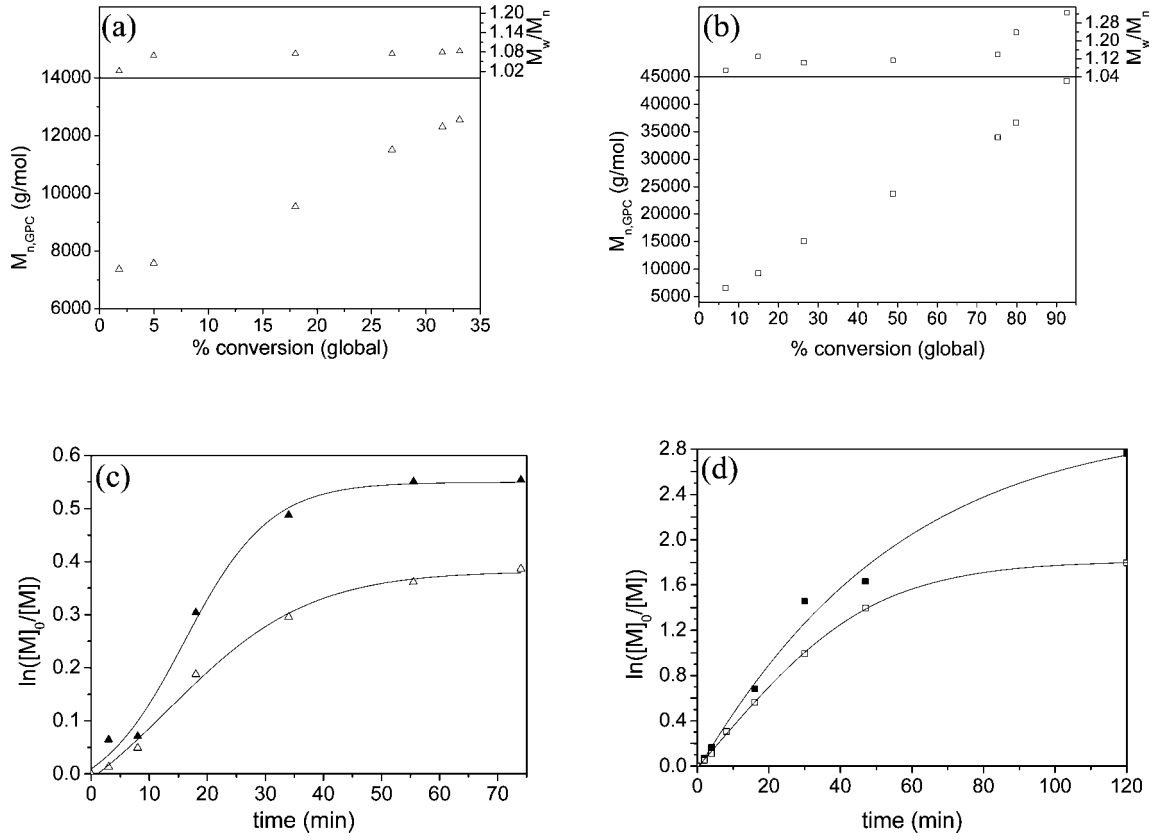

Figure 3. (a) M_n (bottom) and M_w/M_n (top) vs % global conversion for poly(*t*BA-*co*-$PMVE_{16}$-A) **6** (△). (b) M_n (bottom) and M_w/M_n (top) vs % global conversion for poly(*t*BA-*co*-$PMVE_{16}$-A) **8** (□). (c) First-order kinetic plot for the ATRP copolymerization of 10/90 mol % *t*BA/$PMVE_{16}$-A in the feed for poly(*t*BA-*co*-$PMVE_{16}$-A) **6** (▲, △). (d) First-order kinetic plot for the ATRP copolymerization of 90/10 mol % *t*BA/$PMVE_{16}$-A in the feed for poly(*t*BA-*co*-$PMVE_{16}$-A) **8** (■, □). Filled symbols: data for *t*BA; open symbols: data for $PMVE_{16}$-A.

n_D(P*t*BA) = 1.46.[47] By rearranging eq 1, it is possible to calculate the conversion of the macromonomer with the formula

$$\text{conversion}_{\text{PMVE-A}} = \frac{1 - AB \cdot \text{conversion}_{t\text{BA}}}{A + 1} \qquad (2)$$

with A = GPC area$_{\text{PMVE-A}}$/GPC area$_{\text{copolymer}}$ and $B = ([t\text{BA}]_0\text{-}MW_{t\text{BA}}R_2)/([\text{PMVE-A}]_0MW_{\text{PMVE-A}}R_1)$. For some of the reactions in Table 3, the conversion calculation by combination of GC and GPC via the Gladstone−Dale formula was cross-checked by ^{1}H NMR. As can be seen from the data, the results are comparable within the experimental error margin.

The kinetic study of reactions **6** ([*t*BA]:[$PMVE_{16}$-A] = 10:90) and **8** ([*t*BA]:[$PMVE_{16}$-A] = 90:10) is shown in Figure 3. Low polydispersities and a linear evolution of M_n as a function of the global conversion are observed.

Together with the first-order kinetic plots (Figure 3c,d), it can be concluded that the ATRP copolymerization of *t*BA with $PMVE_{16}$-A macromonomer is controlled up to certain conversions, after which the linearity in the first-order plot is lost due to increased steric hindrance and viscosity. As could be expected, this effect is more pronounced for the reaction with the highest amount (90 mol %) of $PMVE_{16}$-A macromonomer in the feed (poly(*t*BA-*co*-$PMVE_{16}$-A) **6** in Figure 3c). Furthermore, the first-order kinetic plots of both reactions demonstrate faster consumption of *t*BA than the $PMVE_{16}$-A macromonomer.

Since reactions **6** and **8** involve the use of a large excess of one monomer relative to the other one, the Mayo and Lewis method[48] simplified by Jaacks[49] was preferentially applied to estimate the relative reactivity of *t*BA and $PMVE_{16}$-A. The

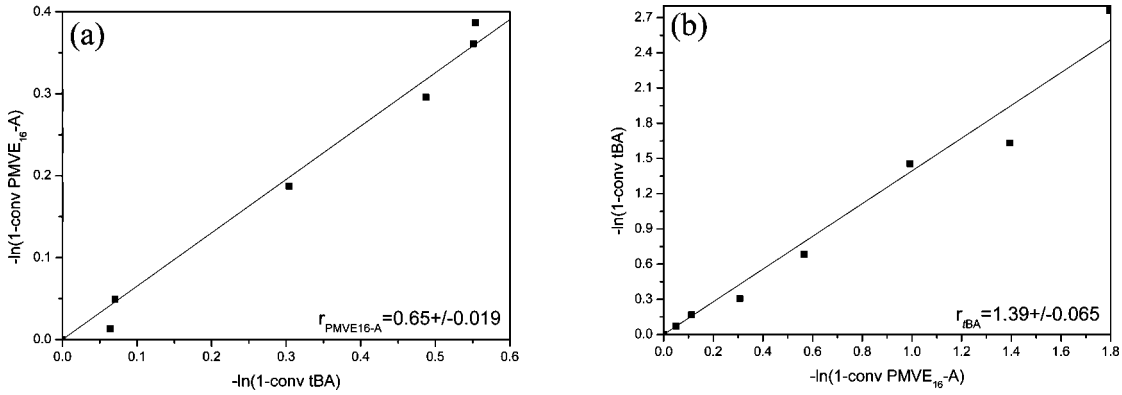

Figure 4. Jaacks plots for the ATRP copolymerization (DP_{total} = 300) of (a) 10/90 mol % tBA/$PMVE_{16}$-A for poly(tBA-*co*-$PMVE_{16}$-A) **6** and (b) 90/10 mol % tBA/$PMVE_{16}$-A for poly(tBA-*co*-$PMVE_{16}$-A) **8**.

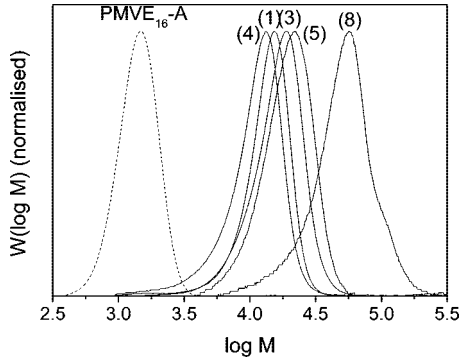

Figure 5. GPC traces (refractive index detection) for $PMVE_{16}$-A macromonomer (---) and poly(*t*BA-*co*-$PMVE_{16}$-A) **4**, **1**, **3**, **5**, and **8** (—) in Table 3.

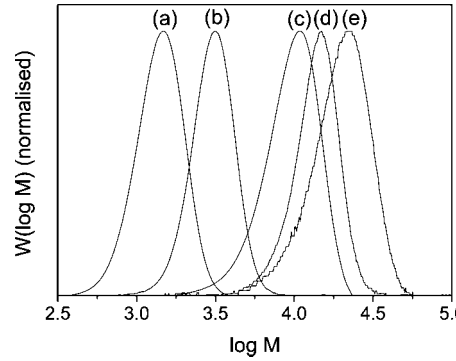

Figure 6. GPC traces (refractive index detection) for (a) $PMVE_{16}$-A macromonomer, (b) P*t*BA_{23} macroinitiator, (c) P*t*BA_{23}-*b*-poly-$(PMVE_{16})_{7.5}$, (d) P*t*BA_{23}-*b*-poly$(PMVE_{16})_{18}$, and (e) P*t*BA_{23}-*b*-poly-$(PMVE_{16})_{32}$.

reactivity ratio of the monomer in excess is obtained from the linear logarithmic plot of comonomer conversions:

$$\ln \frac{[M_1]_t}{[M_1]_0} = r_1 \ln \frac{[M_2]_t}{[M_2]_0} \quad (3)$$

If the conversions of M_1 and M_2 at the time t are C_1 and C_2, respectively, eq 3 can be written as

$$\ln(1 - C_1) = r_1 \ln(1 - C_2) \quad (4)$$

Figure 4a,b shows double-logarithmic plots of fractional comonomer conversions $C_{t\mathrm{BA}}$ and $C_{\mathrm{PMVE_{16}\text{-}A}}$: their slopes provide reactivity ratios $r_{\mathrm{PMVE_{16}\text{-}A}} = 0.65 \pm 0.019$ (Figure 4a) and $r_{t\mathrm{BA}} = 1.39 \pm 0.065$ (Figure 4b). This indicates the formation of copolymers poly(*t*BA-*co*-$PMVE_{16}$-A) with a slight gradient in composition along the backbone of the copolymer, which means that $PMVE_{16}$-A side chains are less concentrated at the beginning of the polymer chain. The reactivity parameters obtained are apparent values, which enclose different experimental parameters, like the inherent reactivity of the vinyl function of the macromonomer, the diffusion of the macromonomer in the reaction medium, and the thermodynamic incompatibility between the growing polymer chain and the macromonomer.[23–25,33]

The GPC curves of some copolymers, after removal of the unreacted (macro)monomer by dialysis against water, are presented in Figure 5. Well-defined copolymers were formed with narrow polydispersities, which indicates that every polymer chain has about the same number and distribution of the grafts. From Table 3, it can further be concluded that copolymerizations with a low targeted degree of polymerization (DP 50 vs DP 300) need less catalyst in order to achieve an acceptable conversion. Indeed, at higher DP, there is increased steric hindrance and a lower radical concentration in the reaction mixture. This reduced reactivity was compensated by the use of a higher catalyst concentration.[32]

Palm-Tree Architectures Based on a P*t*BA and PMVE-A Macromonomer. Not only statistical graft copolymers, but also block copolymers, were prepared with *t*BA and PMVE-A macromonomer. Therefore, well-defined P*t*BA-Br macroinitiators were first prepared by ATRP[38] and subsequently used to initiate ATRP of PMVE-A in a next step (Scheme 1C). This strategy results in the formation of so-called palm-tree block copolymers,[18] also called tadpole-shaped[19] block copolymers. The right reaction conditions for the synthesis of palm-tree block copolymers consisting of P*t*BA and $PMVE_{16}$-A were established using the knowledge buildup during the homopolymerization of $PMVE_{16}$-A and the statistical copolymerization. As the macromonomer is slightly less reactive than a low molecular weight acrylate monomer (see copolymerization parameters), a high reactivity has to be ensured. Therefore, on one hand, the strong ligand Me_6TREN is used and, on the other hand, the catalyst concentration is increased.

As can be concluded from Table 4, palm-tree block copolymers with varying compositions and narrow polydispersities can be prepared by variation of the molecular weight of the P*t*BA macroinitiator, namely P*t*BA_{23} (M_n = 3100 g/mol) and P*t*BA_{51} (M_n = 6700 g/mol), and/or variation of the targeted DP's and the catalyst amounts. The GPC traces in Figure 6 show that the signal of the palm-tree block copolymer quantitatively shifts to higher molecular weights compared to the P*t*BA macroinitiator and that all unreacted macromonomer can be successfully removed by dialysis against water.

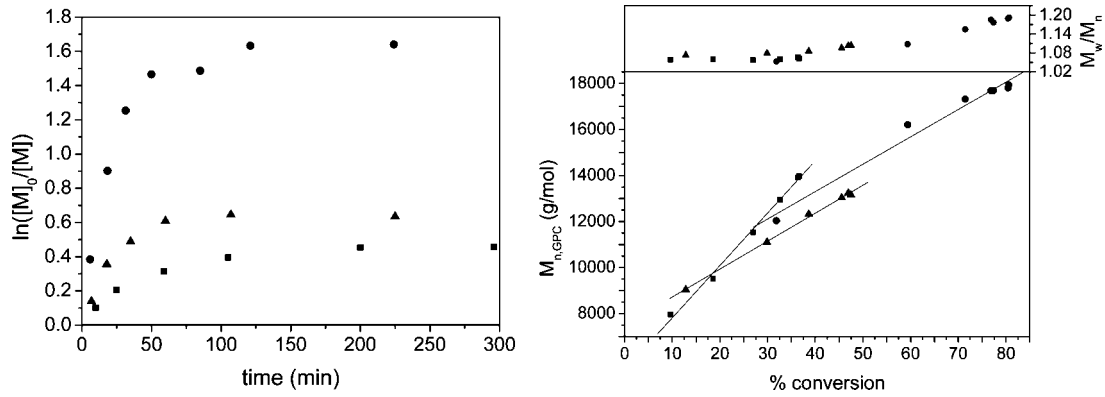

Figure 7. kinetic plots of (a) $\ln([M]_0/[M])$ vs reaction time and (b) dependence of molecular weights (bottom) and molecular weight distributions (top) of the monomer conversion for ATRP of $PMVE_{16}$-A with P*t*BA-Br as a macroinitiator: P*t*BA_{23}-*b*-poly$(PMVE_{16})_{14}$ (■); P*t*BA_{23}-*b*-poly$(PMVE_{16})_{18}$ (▲),and P*t*BA_{23}-*b*-poly$(PMVE_{16})_{32}$ (●).

As for the synthesis of polymacromonomers and for statistical copolymerizations, a deviation from linearity in the first-order kinetic plot occurs (Figure 7a). By increasing the reactivity of the system, it is possible to push the reaction to higher conversions. This could be achieved via several methods: (i) increase of the reaction temperature from 50 to 90 °C; (ii) increase of the catalyst concentration from 1 to 2 equiv (P = *t*BA_{23}-*b*-poly$(PMVE_{16})_{18}$ vs P*t*BA_{23}-*b*-poly$(PMVE_{16})_{32}$); (iii) increase of the radical concentration by starting from a lower $[M]_0/[I]_0$ ratio, in combination with 2 equiv of catalyst. In order to avoid termination reactions by the high radical concentration at the beginning of the reaction, 5 mol % $Cu(II)Br_2$ was added (P*t*BA_{23}-*b*-poly$(PMVE_{16})_{7.5}$). Moreover, the effect of steric hindrance around the growing radical is smaller for lower initial DP's. (iv) The solvent was varied (acetone or toluene). Solvents have a major influence on the polymerization rate and the degree of control in ATRP.[50–53] This is ascribed to the formation of different complex structures, but also to the different solubility of activator and deactivator in several solvents.[54] The more polar solvent acetone promotes the solubility of the catalyst system compared to toluene, such that higher conversions are achievable. The high conversion for P*t*BA_{23}-*b*-poly$(PMVE_{16})_{32}$ can thus probably be attributed not only to the amount of catalyst but also to the use of a polar solvent. Those effects are clearly visible in the first-order kinetic plots (Figure 7a) for the first three reactions in Table 4. Figure 7b shows that M_n evolves linearly as a function of the conversion and that the polydispersities are low. It can thus be concluded that the reactions are controlled up to a certain conversion.

Similarly to the P*t*BA_{23} macroinitiator, an increased conversion can be achieved for the P*t*BA_{51} macroinitiator by increasing the catalyst and radical concentration by starting with a lower targeted DP (P*t*BA_{51}-*b*-poly$(PMVE_{16})_{17}$ vs P*t*BA_{51}-*b*-poly$(PMVE_{16})_{26}$).

Hydrolysis of P*t*BA to PAA. The polymer architectures containing P*t*BA were converted via hydrolysis of the *tert*-butyl groups to pH-sensitive PAA copolymers. Hydrolysis was done with 5 equiv of $MeSO_3H$ relative to the *tert*-butyl ester functions. It was first verified whether the PMVE−ether bonds and the ester linkage between the PMVE chains and the backbone survive those hydrolysis conditions. To this end, the $PMVE_{16}$-A macromonomer was subjected to a model reaction, which consists in the addition of a large excess of $MeSO_3H$ (5 equiv per MVE unit, i.e., 80 equiv per ester linkage). The mixture was stirred for 1 h in CH_2Cl_2 at room temperature. GPC analysis (see Supporting Information, Figure S2a) gives a signal at the same molecular weight as before hydrolysis. Also in MALDI-TOF and ^1H NMR no side products are observed (see Supporting Information, Figure S2b). Successful hydrolysis of the PMVE/P*t*BA copolymers is proven in the same way as previously for the linear block copolymers.[14] In FT-IR the typical asymmetric doublet caused by the *tert*-butyl groups at 1368 and 1393 cm^{-1} disappears, and a broad carboxylic acid band appears in the region 3700–2300 cm^{-1}. In ^1H NMR the *tert*-butyl signal at 1.44 ppm disappears after hydrolysis (see Supporting Information, Figure S3). In order to make GPC analysis of PAA containing copolymers feasible, GPC was measured with *N,N*-dimethylacetamide (with 0.21% LiCl and 0.6% HOAc) as the eluent, following the procedure of Pasch et al.[55] This method allows to reduce ionic and adsorption effects of PAA on the column. The polydispersity index of the samples before and after hydrolysis remains nearly unchanged, which indicates that the characteristics of the polymers are preserved during reaction with 5 equiv of $MeSO_3H$ (see Supporting Information, Figure S4).

Table 5. T_{cp} Values of PolyPMVE (1 wt % Aqueous Solutions, Heating at 0.2 °C/min)

code	$M_{n,exp}$ (g/mol)	T_{cp} (°C)
$PMVE_{16}$-A	1 100	24.9
poly$(PMVE_{16}$-A$)_{17}$	19 200	24.9
poly$(PMVE_{16}$-A$)_{23}$	25 300	23.8

Properties

Temperature-Sensitive (Co)polymers. *PMVE-A Macromonomer and Poly(PMVE) Polymacromonomer.* The temperature-responsive behavior of the PMVE macromononomer and of the poly(PMVE) homopolymers was studied (Table 5). Compared to nonfunctionalized PMVE with a cloud point temperature (T_{cp}) around body temperature (37 °C), $PMVE_{16}$-A shows a lower T_{cp} (24.9 °C), measured by turbidimetry (UV–vis). As published earlier,[56] terminal modification by hydrophobic end groups (coming from the inimer in this case) lowers T_{cp}. In fact, PMVE-A can be considered as an amphiphilic structure composed of a long hydrophilic PMVE block (with narrow polydispersity) and a short hydrophobic block (monodisperse, 14.4 wt %) coming from the inimer. As the molar ratio of the end groups relative to PMVE remains identical in the graft copolymer compared to the PMVE macromonomer, the T_{cp} will also be influenced by the hydrophobic end groups composing the backbone. As can be seen from Table 5, the T_{cp} of the polymacromonomer is of the same order of magnitude as the one of the macromonomer. The influence of the molecular weight ($M_{n,exp}$) on the T_{cp} is according to the expectations for a type III LCST polymer:[56] a higher molecular weight polymer results in a lower T_{cp}.

PtBA-b-PMVE, PtBA-b-poly(PMVE), and Poly(tBA-co-PMVE). In the next section, the influence of the hydrophobic P*t*BA segment on the thermoresponsive properties of PMVE is

Table 6. T_{cp} Values for Different Copolymer Architectures Based on P*t*BA and PMVE

code[a]	mol % P*t*BA	wt % P*t*BA	T_{cp} (°C)
linear block copolymers			
$PMVE_{50}$-Br	0	0	27
$PtBA_{16}$-*b*-$PMVE_{74}$	17	32	26.9
$PtBA_{16}$-*b*-$PMVE_{50}$	24	41	<3 °C[b]
$PtBA_{16}$-*b*-$PMVE_{33}$	32	51	not soluble
palm-tree block copolymers			
$PMVE_{16}$-A	0	0	24.9
$PtBA_{23}$-*b*-poly($PMVE_{16}$-A)$_{32}$	46	9	24.3
$PtBA_{23}$-*b*-poly($PMVE_{16}$-A)$_{18}$	56	13	24.3
$PtBA_{23}$-*b*-poly($PMVE_{16}$-A)$_{14}$	62	16	25.2
$PtBA_{23}$-*b*-poly($PMVE_{16}$-A)$_{7.5}$	76	27	21.8
statistical graft copolymers			
$PMVE_{16}$-A	0	0	24.9
poly(*t*BA-*co*-$PMVE_{16}$) **5**	19	2.6	22.0
poly(*t*BA-*co*-$PMVE_{16}$) **1**	37	6.5	17.3
poly(*t*BA-*co*-$PMVE_{16}$) **3**	58	14	16.0
poly(*t*BA-*co*-$PMVE_{16}$) **4**	79	31	14.5
poly(*t*BA-*co*-$PMVE_{16}$) **8**	92	56	not soluble

[a] Subscripts represent DP. [b] The polymer is dissolved, but it gives a milky solution in the fridge at 3 °C, rendering the measurement of T_{cp} impossible.

described. The T_{cp} values measured for different copolymer architectures with varying compositions of P*t*BA and PMVE are presented in Table 6. The linear block copolymer $PtBA_{16}$-*b*-$PMVE_{74}$[14] shows a lower T_{cp} (27 °C) compared to the value expected for pure PMVE (37 °C). Pure $PMVE_{50}$ prepared with dual initiator 2-bromo-(3,3-diethoxypropyl)-2-methylpropanoate (represented as $PMVE_{50}$-Br; 7.9 wt % hydrophobic end groups) shows a similar T_{cp} decrease. In the block copolymer, however, PMVE has a higher DP, namely DP = 74. This means that for $PMVE_{74}$-Br homopolymer a slightly higher T_{cp} can be expected (than for $PMVE_{50}$-Br) due to the higher ratio of hydrophilic PMVE vs hydrophobic end group. The incorporation of 32 wt % hydrophobic P*t*BA only marginally decreases the LCST of $PMVE_{74}$-Br. However, linear block copolymers P*t*BA-*b*-PMVE with higher fractions of P*t*BA are too hydrophobic and not water-soluble anymore above 3 °C.

For palm-tree block copolymers, the same phenomenon is observed as for the linear block copolymers: incorporation of P*t*BA has, within the experimental error margins, nearly no influence on the T_{cp} of the PMVE-A macromonomer. In the case of a statistical graft copolymer, however, copolymer poly(*t*BA-*co*-$PMVE_{16}$-A) **4** with a comparable P*t*BA content (31 wt %) gives a much larger T_{cp} decrease (±10 deg) compared to the T_{cp} of the PMVE macromonomer. Similar results for block and graft copolymers based on poly(*N*-isopropylacrylamide) as temperature-sensitive polymer with a hydrophobic segment ($C_{18}H_{35}$, polystyrene, or methacrylic acid stearyl ester) were reported in the literature.[57–59]

The fact that the T_{cp} for the amphiphilic block copolymers (linear and palm tree) is nearly independent of the comonomer fraction can be explained by the fact that the P*t*BA chains are not directly interacting with the PMVE chains in aqueous medium. Micelle formation (see further, Figure 8b,d) occurs through self-aggregation of the hydrophobic segments of the block copolymer, excluding the water molecules from the hydrophobic core of the micelle.[60,61] As P*t*BA in the core of the micelle is protected from the water by PMVE, the P*t*BA segments give (nearly) no hydrophobic contribution to the LCST.[57–59,62] On the contrary, for the statistical graft copolymers, no micelle formation is expected as hydrophobic aggregation of the comonomer causes partial entanglement of the temperature sensitive polymer[63] (Figure 8f). Consequently, the hydrophobic aggregates remain partially exposed to water and influence the T_{cp} value more strongly. This phenomenon was already observed earlier by Patrickios et al.[63] for a statistical terpolymer of hexa(ethylene glycol) methacrylate, *N,N′*-(dimethylamino)ethyl methacrylate, and methyl methacrylate. In order to verify whether this micellar aggregation theory is correct, the micellization of block and statistical copolymers was compared via ^{1}H NMR in selective solvents. This technique is a common method to observe micellar aggregation, as demonstrated by Spevacek,[64] Armes,[65–67] and others.[68–70] As a point of reference, ^{1}H NMR spectra are measured in a good solubilizing solvent ($CDCl_3$) for both P*t*BA and PMVE. D_2O was used as a selective solvent for PMVE. Since micelles can only be formed if the block copolymers are amphiphilic, ^{1}H NMR spectra have to be measured below the T_{cp} of PMVE (5 °C was chosen). If micellization occurs with the formation of a hydrophobic P*t*BA core, protected from D_2O by the surrounding hydrophilic PMVE corona, a disappearance, or at least a decrease in relative intensity (compared to ^{1}H NMR in the good solvent $CDCl_3$), of the P*t*BA signals should be observed. The ^{1}H NMR spectra confirm the assumption that the block copolymers (linear and palm tree) form micelles, while the statistical copolymers do not. Indeed, for the linear and palm-tree block copolymers the typical P*t*BA peaks disappear in D_2O at 5 °C (Figure 8a−d). In the case of statistical copolymers, there is no indication of micelle formation because the signals of P*t*BA remain clearly visible in the selective solvent, with approximately the same relative integrations as in the common solvent $CDCl_3$ (Figure 8e,f).

pH- and Temperature-Sensitive Copolymers. In order to study the biresponsive behavior, some of the P*t*BA/PMVE containing copolymers were hydrolyzed to the corresponding polymers composed of PAA/PMVE (Table 7).

T_{cp} Study as a Function of pH by Turbidimetry (UV–vis). As PAA is pH-sensitive and PMVE temperature-sensitive, the influence of the pH on the ionization of PAA has to be considered for the study of the LCST of PMVE. Therefore, the different samples were dissolved in buffers of pH 2−10, and the T_{cp} of those 1 wt % aqueous solutions was determined by turbidimetry (UV–vis). Figure 9a shows the typical course of the variation in light absorbance at 540 nm as a function of the temperature for 1 wt % buffered PAA_{16}-*b*-$PMVE_{74}$ solutions (pH 2−9). A T_{cp} is observed at all pH values and the absorbance curves shift to a higher temperature starting from a pH between 4 and 5. The T_{cp} values of those linear block copolymers are shown as a function of the pH in Figure 9b. Similar to the shift of the absorbance curves to higher temperatures in Figure 9a, a T_{cp} jump occurs between pH 4 and 5 in Figure 9b, which can be correlated with the pK_a of PAA. Below the pK_a value, a decrease in the T_{cp} of the block copolymers is observed compared to the T_{cp} of pure PMVE-Br (~30 °C for DP = 50–74, see Table 6). If the pH decreases, the ratio of nonionized COOH groups vs the ionized acid groups (COO^-) in PAA increases, which makes the formation of inter- and intramolecular hydrogen bonds between PAA and PMVE[14] more probable. This results in a decrease of the PMVE−water interactions, and as a consequence in a decrease of the hydrophilic nature of the copolymers (thus a T_{cp} decrease). Logically, it can be expected that this T_{cp} decrease will be larger if the polymer becomes more hydrophobic, i.e., if the polymer contains more PAA that can form hydrogen bonds with PMVE. This is indeed observed when the results at pH 4 for both block copolymer samples in Figure 9b are compared.

At lower pH however, the T_{cp} values of both samples are close to each other. This is ascribed to the fact that the samples are not completely water-soluble at this low pH due to complexation, and the fraction of insoluble polymer increases for larger PAA fractions. From the type III phase diagram of PMVE,[56] it can be deduced that the T_{cp} is higher for lower polymer concentrations. Indeed, a higher water content induces

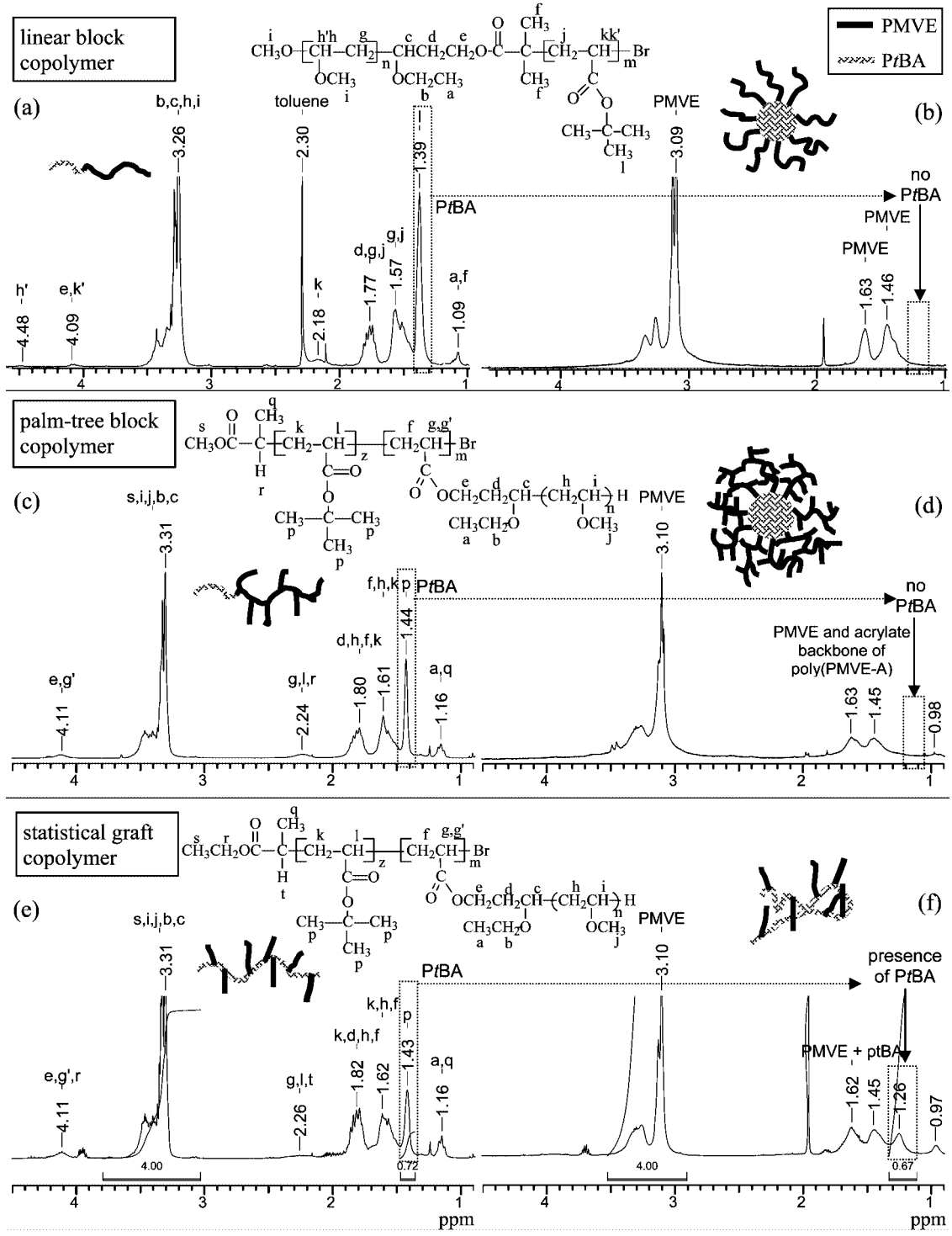

Figure 8. ^{1}H NMR in different solvents: (a) P*t*BA$_{16}$-*b*-PMVE$_{74}$ in $CDCl_3$ (300 MHz), (b) P*t*BA$_{16}$-*b*-PMVE$_{74}$ in D_2O at 5 °C (500 MHz), (c) P*t*BA$_{23}$-*b*-poly(PMVE$_{16}$-A)$_{14}$ in $CDCl_3$ (300 MHz), (d) P*t*BA$_{23}$-*b*-poly(PMVE$_{16}$-A)$_{14}$ in D_2O at 5 °C (500 MHz), (e) poly(*t*BA-*co*-PMVE$_{16}$-A) **3** in $CDCl_3$ (300 MHz), and (f) poly(*t*BA-*co*-PMVE$_{16}$-A) **3** in D_2O at 5 °C (500 MHz).

more polymer/water interactions, and by consequence more thermal energy is required in order to break the water structure, such that hydrophobic polymer/polymer interactions (i.e., precipitation) can dominate over polymer/water interactions.[71] The constant T_{cp} at low pH values could also be due to micelle formation as in the case of the P*t*BA-PMVE copolymers, where it was shown that the weight fraction of P*t*BA does not influence much the T_{cp}.

With increasing pH, the COOH:COO^- ratio decreases, which causes a decrease of the hydrogen-bonding contribution and an increase in the hydrophilicity of the PMVE/PAA copolymers. Above its pK_a, PAA is fully ionized (hydrophilic), and the carboxylic acid groups repel each other electrostatically. This results in a T_{cp} increase, proportional to the hydrophilicity (wt % PAA) of the copolymers: at pH 9 the T_{cp} of PAA$_{16}$-*b*-PMVE$_{74}$ with 21 wt % PAA (■) is smaller than the T_{cp} of PAA$_{16}$-*b*-PMVE$_{50}$ with 28 wt % PAA (△). Müller et al. did similar observations for another biresponsive block copolymer, namely poly(*N*-isopropylacrylamide-*b*-acrylic acid).[5]

The transition between complexed COOH groups and free carboxylate (COO^-) at increasing pH was confirmed for different polymer architectures via FT-IR at pH 3 and pH 10

Table 7. Data for the PAA/PMVE Containing Copolymer Architectures Derived from the Corresponding P*t*BA/PMVE Precursors in Table 6

code	mol % PAA	wt % PAA
linear block copolymers		
PAA_{16}-*b*-$PMVE_{74}$	17	21
PAA_{16}-*b*-$PMVE_{50}$	24	28
statistical copolymers		
poly(AA-*co*-$PMVE_{16}$) **1**	37	4
poly(AA-*co*-$PMVE_{16}$) **3**	58	8
poly(AA-*co*-$PMVE_{16}$) **4**	79	20
poly(AA-*co*-$PMVE_{16}$) **8**	92	42
palm-tree block copolymers		
PAA_{23}-*b*-poly($PMVE_{16}$-A)$_{32}$	46	5
PAA_{23}-*b*-poly($PMVE_{16}$-A)$_{18}$	56	8
PAA_{23}-*b*-poly($PMVE_{16}$-A)$_{7.5}$	76	17

(Figure 10). At pH 3, the peak around 1738 cm^{-1} demonstrates that the COOH groups form hydrogen bonds. Upon increase of the pH, this peak diminishes and a carboxylate peak around 1575 cm^{-1} appears, indicating that the hydrogen bonds are broken at high pH.

Among the statistical graft copolymers obtained by copolymerization of $PMVE_{16}$-A macromonomer, only the copolymers with high PAA content (20 and 42 wt %) contain a precipitate at low pH. The expected T_{cp} decrease with increasing PAA content (and thus increasing complexation) is now clearly observed at low pH (Figure 9c). At high pH the general rule holds that copolymers of PMVE with hydrophilic comonomers have a higher T_{cp} compared to the $PMVE_{16}$-A macromonomer. A larger hydrophilic part allows the copolymer to stay in solution up to a higher temperature. For poly(AA-*co*-$PMVE_{16}$-A) **8** with 42 wt % PAA, a T_{cp} could only be measured at pH 4. At a lower pH the polymer is not water-soluble anymore, and at higher pH no T_{cp} was observed up to 80 °C, which means that the T_{cp} at pH 4 must be situated in the pH jump. From these observations, it can be concluded that the temperature-sensitive behavior of PMVE is lost above a critical amount of PAA.

The aqueous samples of the palm-tree block copolymers based on $PMVE_{16}$-A macromonomer (Figure 9d) with a small amount of PAA are fully water-soluble over the whole pH range, but PAA_{23}-*b*-poly($PMVE_{16}$-A)$_{7.5}$ with 17 wt % PAA (■) gives precipitate formation at pH 2 and pH 3. Nevertheless, at low pH the expected trend is visible: T_{cp} decreases as the polymer contains more PAA (Figure 9d). At high pH, however, T_{cp} does not increase as a function of the number of PAA units in the copolymer, as was the case for the linear block copolymers and statistical copolymers. At high pH the T_{cp} of the palm-tree block copolymers is of the same order of magnitude than the T_{cp} of the $PMVE_{16}$-A macromonomer.

The fact that polymers with comparable compositions but different architecture (PAA_{16}-*b*-$PMVE_{74}$, PAA_{23}-*b*-poly($PMVE_{16}$-A)$_{7.5}$, and poly(AA-*co*-$PMVE_{16}$-A) **4** with ~20 wt % PAA) show fundamentally different phase separation behavior suggests that their supramolecular structures differ. The common point between the different copolymer architectures is that a T_{cp} jump occurs as a function of pH and that it occurs at lower pH (closer to the pK_a value of pure PAA) for higher PAA contents. Moreover, the T_{cp} jump covers a larger temperature range for copolymers with a larger PAA fraction.

Dynamic Light Scattering (DLS). Dilute solutions (concentration ≈ 1.6 g/L) of selected copolymers (poly($PMVE_{16}$)$_{17}$, PAA_{16}-*b*-$PMVE_{74}$, poly(AA-*co*-PMVE) **3**, and PAA_{23}-*b*-($PMVE_{16}$)$_7$) have been prepared in buffered water. Details about sample preparation can be found in the Experimental Part. Because of technical problems (water condensation at low temperature), no reliable DLS measurements could be obtained

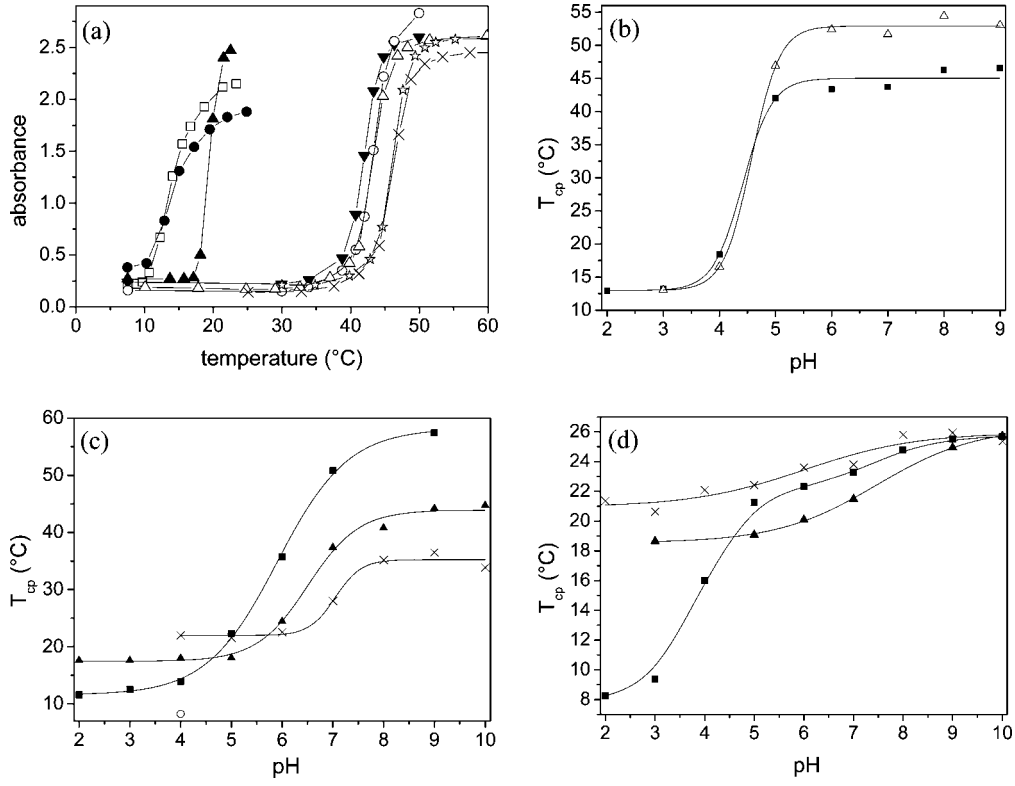

Figure 9. (a) UV–vis absorbance curves as a function of temperature for 1 wt % buffered PAA_{16}-*b*-$PMVE_{74}$ solutions at pH 2 (□), pH 3 (●), pH 4 (▲), pH 5 (▼), pH 6 (○), pH 7 (△), pH 8 (☆), and pH 9 (×). (b) T_{cp} vs pH for linear block copolymers PAA_{16}-*b*-$PMVE_{74}$ with 21 wt % PAA (■) and PAA_{16}-*b*-$PMVE_{50}$ with 28 wt % PAA (△). (c) T_{cp} vs pH for statistical graft copolymers poly(AA-*co*-$PMVE_{16}$-A) with 4 wt % PAA (×), 8 wt % PAA (▲), 20 wt % PAA (■), and 42 wt % PAA (○). (d) T_{cp} vs pH for palm-tree block copolymers PAA_{23}-*b*-poly($PMVE_{16}$-A)$_{32}$ with 5 wt % PAA (×), PAA_{23}-*b*-poly($PMVE_{16}$-A)$_{18}$ with 8 wt % PAA (▲), and PAA_{23}-*b*-poly($PMVE_{16}$-A)$_{7.5}$ with 17 wt % PAA (■).

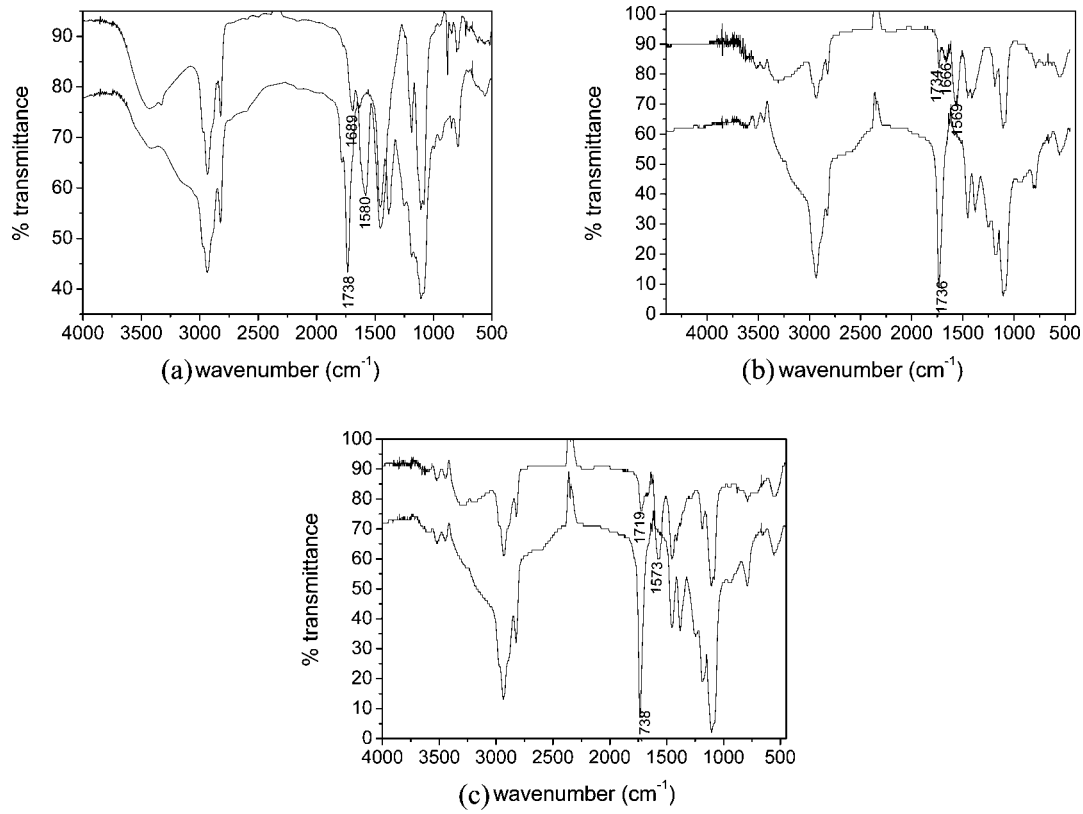

Figure 10. FT-IR spectra at pH 10 (top) and pH 3 (bottom) for (a) PAA_{16}-*b*-$PMVE_{74}$, (b) PAA_{51}-*b*-poly($PMVE_{16}$-A)$_{26}$, and (c) poly(AA-*co*-$PMVE_{16}$-A) **4** with 20 wt % PAA.

Table 8. Dynamic Light Scattering Results of the Different Buffered (pH 10) Solutions of Copolymers below and above the Cloud Point[a]

polymer	R_h (nm) at 20 °C	R_h (nm) at 55 °C
poly($PMVE_{16}$)$_{17}$ comb-shaped	17 (0.50)	768 (0.30)
PAA_{16}-*b*-$PMVE_{74}$ linear block copolymer	54 (0.48)	258 (0.31)
PAA_{23}-*b*-poly($PMVE_{16}$)$_{7.5}$ palm-tree block copolymer	71 (0.10)	324 (0.50)
poly(AA-*co*-PMVE) **3** statistical graft copolymer	63 (0.35)	123 (0.20)

[a] The PDI are given in parentheses.

for the samples at pH 3 at low temperature. The results for pH 10 are summarized in Table 8.

First of all, it should be noted that aggregates have been detected in all the starting solutions at 20 °C, although all samples should exist as unimers at this temperature since they only contain hydrophilic groups. The hydrodynamic radius (R_h) of these aggregates is about 17 nm for the poly($PMVE_{16}$)$_{17}$ sample while it is ca. 60 nm for the copolymers containing PAA blocks (Table 8). The formation of aggregates in poly ($PMVE_{16}$)$_{17}$ could be attributed to defects in the hydrogen-bonded network of water molecules around PMVE blocks, which could create hydrophobic microenvironments acting as association points. The crowded brushlike structure with the acrylate backbone of the poly($PMVE_{16}$)$_{17}$ sample could also be in part responsible of these defects. In the case of PAA-containing copolymers, the aggregation could be due to the well-known and earlier explained polyelectrolyte effect since the PAA is charged at this pH.[72] After crossing the cloud point, very large particles were observed (more than 700 nm) in the case of the poly($PMVE_{16}$)$_{17}$ sample, in agreement with the observed macroscopic precipitation. For the PAA-containing samples, objects with a R_h of about 150–300 nm were observed (Table 8). Such huge R_h's are not in agreement with the formation of block copolymer micelles but rather indicate the formation of stable colloidal aggregates. The reversible formation of those aggregates has been confirmed by DLS for all systems under investigation.

Conclusions

This paper describes the combination of living cationic polymerization and controlled radical polymerization (ATRP) to generate several (co)polymer architectures using the inimer strategy. Acrylate-functionalized PMVE macromonomer was successfully prepared by living cationic polymerization of MVE with inimer 3,3-diethoxypropyl acrylate. PMVE macromonomers were homo and (block) copolymerized with *tert*-butyl acrylate (precursor for acrylic acid) via ATRP, yielding comb polymers, statistical graft copolymers, and palm-tree block copolymers. Palm-tree block copolymers were successfully prepared starting from a P*t*BA-Br (made by ATRP) macroinitiator. Copolymerization of PMVE-A with a monomer such as *t*BA results in statistical graft copolymers. Finally, the P*t*BA-segments were transformed via hydrolysis into the pH-responsive PAA.

The influence of the copolymer composition (P*t*BA, PAA) and architecture (comb polymers, linear and palm-tree block copolymers, statistical graft copolymers) on the thermosensitive behavior of the PMVE segments has been studied. Thermosensitive copolymers composed of P*t*BA and PMVE show a T_{cp} behavior that depends on the polymer architecture. Linear and palm-tree block copolymers have a T_{cp} that is nearly independent of the content of hydrophobic P*t*BA, while for statistical graft copolymers the T_{cp} decreases as a function of increasing P*t*BA content. The different behavior of those architectures can be related to the fact that amphiphilic block copolymers (i.e., below

T_{cp}) are able to form micelles, while statistical graft copolymers are not.

For the PAA-containing copolymers, the influence of the pH on the T_{cp} was studied. For both the block copolymers (linear and palm tree) and the statistical graft copolymers, increasing PAA content decreases T_{cp} at low pH compared to the T_{cp} of the PMVE building block due to complexation (hydrogen bonding). At high pH, the T_{cp} seems to depend on the copolymer architecture. Linear block copolymers and statistical graft copolymers show an increase in T_{cp} as the PAA$-COO^-$ content increases (i.e., increasing hydrophilicity). However, for the palm-tree block copolymers the T_{cp} seems not to depend on the PAA content and is comparable to the T_{cp} found for the PMVE macromonomer.

Acknowledgment. K. Bernaerts thanks the FWO (Research Foundation-Flanders) for a PhD scholarship. The ESF program STIPOMAT and the Belgian Programme on Interuniversity Attraction Poles initiated by the Belgian State, Prime Minister office (P6/27), are acknowledged for financial support. C. A. Fustin is Chercheur Qualifié FRS-FNRS. J.C.M gratefully acknowledges the FWO for various NMR equipment grants (G.0036.00N and G.00365.03).

Supporting Information Available: Materials and methods; GPC curves for the ATRP homopolymerization of $PMVE_{16}$-A; model reaction between $MeSO_3H$ and $PMVE_{16}$-A; ^1H NMR and GPC analysis of PMVE/P*t*BA before and after hydrolysis. This material is available free of charge via the Internet at http://pubs.acs.org.

References and Notes

(1) Snowden, M.; Murray, M. J.; Chowdry, B. Z. *Chem. Ind. (London)* **1996**, 531–534.
(2) Dai, L. *Intelligent Macromolecules for Smart Devices: From Materials Synthesis to Device Applications*; Springer-Verlag: London, 2004.
(3) Bernaerts, K. V.; Willet, N.; Van Camp, W.; Jérôme, R.; Du Prez, F. E. *Macromolecules* **2006**, *39*, 3760–3769.
(4) Gil, E. S.; Hudson, S. M. *Prog. Polym. Sci.* **2004**, *29*, 1173–1222.
(5) Schilli, C. M.; Zhang, M.; Rizzardo, E.; Thang, S. H.; Chong, B. Y. K.; Edwards, K.; Karlsson, G.; Müller, A. H. E. *Macromolecules* **2004**, *37*, 7861–7866.
(6) Nurkeeva, Z. S.; Mun, G. A.; Khutoryanskiy, V. V.; Dzhusupbekova, A. B. *Radiat. Phys. Chem.* **2004**, *69*, 205–209.
(7) Shibanuma, T.; Aoki, T.; Sanui, K.; Ogata, N.; Kikuchi, A.; Sakurai, Y.; Okano, T. *Macromolecules* **2000**, *33*, 444–450.
(8) Staikos, G.; Bokias, G.; Karayanni, K. *Polym. Int.* **1996**, *41*, 345–350.
(9) Glavis, F. J. Poly(Acrylic Acid) and its Homologues. In *Water Soluble Resins*; Davidson, R. L., Sittig, M., Eds.; Reinhold Book Corp: New York, 1968.
(10) Matyjaszewski, K.; Xia, J. *Chem. Rev.* **2001**, *101*, 2921–2990.
(11) Kamigaito, M.; Ando, T.; Sawamoto, M. *Chem. Rev.* **2001**, *101*, 3689–3745.
(12) Higashimura, T.; Sawamoto, M. Carbocationic Polymerization: Vinyl Ethers. In *Comprehensive Polymer Science*; Allen, G., Bevington, J., Eds.; Pergamon: Oxford, 1989; Vol. *3*, pp 673–696.
(13) Reyntjens, W. G. S.; Goethals, E. J. *Des. Monomers Polym.* **2001**, *4*, 195–201.
(14) Bernaerts, K. V.; Du Prez, F. E. *Polymer* **2005**, *46*, 8469–8482.
(15) Bernaerts, K. V.; Du Prez, F. E. *Prog. Polym. Sci.* **2006**, *31*, 671–722.
(16) Bernaerts, K. V.; Schacht, E. H.; Goethals, E. J.; Du Prez, F. E. *J. Polym. Sci., Part A: Polym. Chem.* **2003**, *41*, 3206–3217.
(17) Erdogan, T.; Bernaerts, K. V.; Van Renterghem, L. M.; Du Prez, F. E.; Goethals, E. J. *Des. Monomers Polym.* **2005**, *8*, 705–714.
(18) Pirotton, S.; Muller, C.; Pantoustier, N.; Botteman, F.; Collinet, B.; Grandfils, C.; Dandrifosse, G.; Degee, P.; Dubois, P.; Raes, M. *Pharm. Res.* **2004**, *21*, 1471–1479.
(19) Ohno, S.; Matyaszewski, K. *J. Polym. Sci., Part A: Polym. Chem.* **2006**, *44*, 5454–5467.
(20) Yamada, K.; Miyazaki, M.; Ohno, K.; Fukuda, T.; Minoda, M. *Macromolecules* **1999**, *32*, 290–293.
(21) Guo, Y.; Wang, T.; Zou, Y.; Pan, C. *Polymer* **2001**, *42*, 6385–6391.
(22) Shinoda, H.; Matyjaszewski, K. *Macromolecules* **2001**, *34*, 6243–6248.
(23) Lutz, J.-F.; Jahed, N.; Matyjaszewski, K. *J. Polym. Sci., Part A: Polym. Chem.* **2004**, *42*, 1939–1952.
(24) Shinoda, H.; Miller, P. J.; Matyjaszewski, K. *Macromolecules* **2001**, *34*, 3186–3194.
(25) Shinoda, H.; Matyjaszewski, K. *Macromol. Rapid Commun.* **2001**, *22*, 1176–1181.
(26) Shinoda, H.; Matyjaszewski, K.; Okrasa, L.; Mierzwa, M.; Pakula, T. *Macromolecules* **2003**, *36*, 4772–4778.
(27) Mespouille, L.; Degée, P.; Dubois, P. *Eur. Polym. J.* **2005**, *41*, 1187–1195.
(28) Kaneyoshi, H.; Matyjaszewski, K. *J. Appl. Polym. Sci.* **2007**, *105*, 3–13.
(29) Lahitte, J.-F.; Pelascini, F.; Peruch, F.; Meneghetti, S. P.; Lutz, P. J. *C. R. Chim.* **2002**, *5*, 225–234.
(30) Neugebauer, D.; Zhang, Y.; Pakula, T. *J. Polym. Sci., Part A: Polym. Chem.* **2006**, *44*, 1347–1356.
(31) Neugebauer, D. *Polymer* **2007**, *48*, 4966–4973.
(32) Neugebauer, D.; Zhang, Y.; Pakula, T.; Matyjaszewski, K. *Macromolecules* **2005**, *38*, 8687–8693.
(33) Neugebauer, D.; Zhang, Y.; Pakula, T.; Matyjaszewski, K. *Polymer* **2003**, *44*, 6863–6871.
(34) Buathong, S.; Peruch, F.; Isel, F.; Lutz, P. J. *PMSE Prepr.* **2004**, *91*, 328–329.
(35) Karayanni, K.; Staikos, G. *Eur. Polym. J.* **2000**, *36*, 2645–2650.
(36) Cowie, J. M. G.; Garay, M. T.; Lath, D.; McEwen, I. J. *Br. Polym. J.* **1989**, *21*, 81–85.
(37) Nurkeeva, Z. S.; Khutoryanskiy, V. V.; Mun, G. A.; Bitekenova, A. B. *J. Polym. Sci., Ser. B* **2003**, *45*, 365–369.
(38) Vidts, K. R. M.; Dervaux, B.; Du Prez, F. E. *Polymer* **2006**, *47*, 6028–6037.
(39) Qiu, J.; Matyjaszewski, K.; Thouin, L.; Amatore, C. *Macromol. Chem. Phys.* **2000**, *201*, 1625–1631.
(40) Gao, B.; Chen, X.; Ivan, B.; Kops, J.; Batsberg, W. *Macromol. Rapid Commun.* **1997**, *18*, 1095.
(41) Roos, S. G.; Müller, A. H. E.; Matyjaszewski, K. *Macromolecules* **1999**, *32*, 8331–8335.
(42) Tsukahara, Y.; Mizuno, K.; Segawa, A.; Yamashita, Y. *Macromolecules* **1989**, *22*, 1546–1552.
(43) Tsukahara, Y. Macromonomers: characterization, polymerization reactivity and applications. In *Macromolecular Design: Concept and Practice*; Mishra, M. K., Ed.; Polymer Frontiers Int.: New York, 1994; p 182.
(44) Orwoll, R. A. In *Physical Properties of Polymers*; Mark, J. E., Ed.; AIP Press: Woodbury, NY, 1996; Chapter 7.
(45) Seferis, J. C. In *Polymer Handbook*, 4th ed.; Brandrup, J., Immergut, E. H., Grulke, E. A., Eds.; John Wiley & Sons: New York, 1999; p VI. 571.
(46) Hong, S. C.; Jia, S.; Teodorescu, M.; Kowalewski, T.; Matyjaszewski, K.; Gottfried, A. C.; Brookhart, M. *J. Polym. Sci., Part A: Polym. Chem.* **2002**, *40*, 2736–2749.
(47) Elias, H.-G. In *Polymer Handbook*; Brandrup, J., Immergut, E. H., Grulke, E. A., Eds.; John Wiley & Sons: New York, 1999; p III.55.
(48) Mayo, F. R.; Lewis, F. M. *J. Am. Chem. Soc.* **1944**, *66*, 1594–161.
(49) Jaacks, V. *Makromol. Chem.* **1972**, *161*, 161–172.
(50) Matyjaszewski, K.; Nakagawa, Y.; Jasieczek, C. B. *Macromolecules* **1998**, *31*, 1535–1541.
(51) Nanda, A. K.; Matyjaszewski, K. *Macromolecules* **2003**, *36*, 1487–1493.
(52) Nanda, A. K.; Matyjaszewski, K. *Macromolecules* **2003**, *36*, 599–604.
(53) Chambard, G.; Klumperman, B.; German, A. L. *Macromolecules* **2000**, *33*, 4417–4421.
(54) Huang, J.; Pintauer, T.; Matyjaszewski, K. *J. Polym. Sci., Part A: Polym. Chem.* **2004**, *42*, 3285–3292.
(55) Adler, M.; Pasch, H.; Meier, C.; Senger, R.; Koban, H.-G.; Augenstein, M.; Reinhold, G. *e-Polym.* **2004**, *055*, 1–16.
(56) Van Durme, K.; Van Mele, B.; Bernaerts, K. V.; Verdonck, B. V.; Du Prez, F. E. *J. Polym. Sci., Part B: Polym. Phys.* **2006**, *44*, 461–469.
(57) Chung, J. E.; Yokoyama, M.; Aoyagi, T.; Sakurai, Y.; Okano, T. *J. Controlled Release* **1998**, *53*, 119–130.
(58) Chung, J. E.; Yokoyama, M.; Suzuki, K.; Aoyagi, T.; Sakurai, Y.; Okano, T. *Colloids Surf., B* **1997**, *9*, 37–48.
(59) Cammas, S.; Suzuki, K.; Sone, C.; Sakurai, Y.; Kataoka, K.; Okano, T. *J. Controlled Release* **1997**, *48*, 157–164.
(60) Tuzar, Z.; Kratochvil, P. *Adv. Colloid Interf. Sci.* **1976**, *6*, 201–232.
(61) Wilhelm, M.; Zhao, C. L.; Wang, Y. C.; Xu, R. L.; Winnik, M. A.; Mura, J. L.; Riess, G.; Croucher, M. D. *Macromolecules* **1991**, *24*, 1033–1040.
(62) Winnik, F. M.; Davidson, A. R.; Hamer, G. K.; Kitano, H. *Macromolecules* **1992**, *25*, 1876–1880.
(63) Triftaridou, A. I.; Vamvakaki, M.; Patrickios, C. S. *Polymer* **2002**, *43*, 2921–2926.
(64) Spevacek, J. *Makromol. Chem., Rapid. Commun.* **1982**, *3*, 697–703.

(65) Patrickios, C. S.; Forder, C.; Armes, S. P.; Billingham, N. C. *J. Polym. Sci., Part A: Polym. Chem.* **1996**, *34*, 1529–1541.
(66) Forder, C.; Patrickios, C. S.; Armes, S. P.; Billingham, N. C. *Macromolecules* **1996**, *29*, 8160–8169.
(67) Liu, S.; Billingham, N. C.; Armes, S. P. *Angew. Chem., Int. Ed.* **2001**, *40*, 2328–2331.
(68) Riess, G. *Prog. Polym. Sci.* **2003**, *28*, 1107–1170.
(69) Gohy, J.-F. *Adv. Polym. Sci.* **2005**, *190*, 65.
(70) Verdonck, B.; Gohy, J.-F.; Khousakoun, E.; Jérôme, R.; Du Prez, F. *Polymer* **2005**, *46*, 9899–9907.
(71) Verbrugghe, S.; Bernaerts, K.; Du Prez, F. E. *Macromol. Chem. Phys.* **2003**, *204*, 1217–1225.
(72) Förster, S.; Abetz, V.; Müller, A. H. E. *Adv. Polym. Sci.* **2004**, *166*, 173–210.

MA702547G